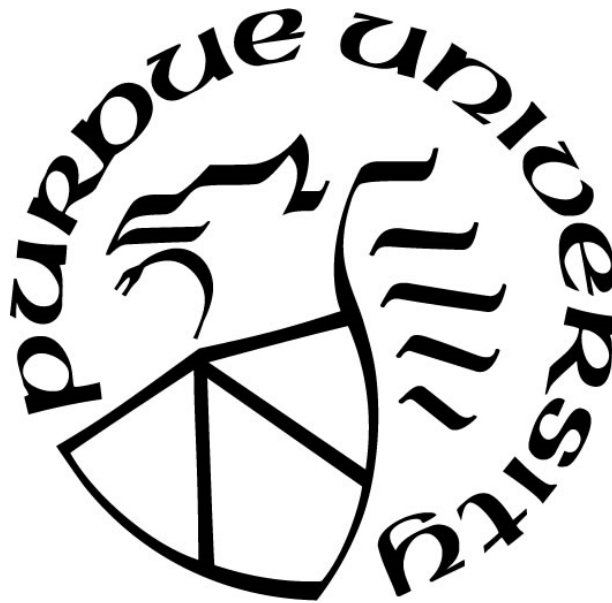# POST-FIRE ASSESSMENT OF CONCRETE IN BRIDGE DECKS

by

Sijia Wang

A Thesis

Submitted to the Faculty of Purdue University

In Partial Fulfillment of the Requirements for the degree of

Master of Science in Civil Engineering

Lyles School of Civil Engineering

West Lafayette, Indiana

August 2019

THE PURDUE UNIVERSITY GRADUATE SCHOOL
STATEMENT OF COMMITTEE APPROVAL

Dr. Amit H. Varma, Chair
 Lyles School of Civil Engineering

Dr. Jan Olek
 Lyles School of Civil Engineering

Dr. Christopher Williams
 Lyles School of Civil Engineering

Approved by:
 Dr. Dulcy M. Abraham
  Head of the Graduate Program

To my grandpa, who taught me the significance of knowledge.

ACKNOWLEDGMENTS

First of all, I would like to thank my advisor, Dr. Amit Varma, for giving me this great opportunity to work on this research project and for all the knowledge, guidance, and assistance that you gave me throughout my undergraduate and graduate study. Working with you on various projects allowed me to gain the experience I would not learn from coursework. I would like to thank Dr. Jan Olek and Dr. Christopher Williams, for serving on my graduate committee and for contributing to my academic and research development. I am grateful for working with you on this project and learning more knowledge from fire, concrete and material areas. I would also like to thank all the professors who taught me in civil engineering at Purdue. Thank you for letting me learn how to become a professional civil engineer.

I would like to thank Tom Bradt for always helping me with setting up my experiments and teaching me about instrumentation installation. I would like to thank Tzu-Chun Tseng for guiding me through this research, helping me with the experiments, as well as always giving me great advice on exploring food options in West Lafayette. I would like to thank Raikhan Tokpatayeva for teaching me all the material analysis methods and showing me how to be professional on material experimental studies. I would like to thank Dan Huang for helping me on the preparations and observations of all the SEM samples and being the best kick-boxing partner. This research would not be completed without all of your help.

I would like to thank my best friends Farida Mahmud, Leslie Bonthron, and Herta Montoya for always keeping me company and sharing joy with me in these two years. I am so grateful that I have met you during my graduate study. I would also like to thank my therapist for listening and talking to me patiently and giving me so many mental supports. Last but not least, thank you to my parents and grandma, for all the support through these six years. Special thanks to Bo Ji for being the best partner I could ever ask for, giving me lots of love and patience throughout my graduate study.

TABLE OF CONTENTS

LIST OF TABLES

LIST OF FIGURES

ABSTRACT

Author: Wang, Sijia. MSCE
Institution: Purdue University
Degree Received: August 2019
Title: Post-Fire Assessment of Concrete in Bridge Decks
Committee Chair: Amit Varma

In recent years, there have been a number of truck fires involving bridges with concrete components. If the fire burns for a significant period of time, the structural integrity of concrete components could be damaged due to fire. Research-based guidance for evaluating the level of fire damage is currently unavailable and would be beneficial for post-fire bridge inspectors.

This research project focused on evaluating the effects of fire induced damage on concrete bridge deck elements. In order to achieve this goal, a series of controlled heating experiments and material analysis were conducted. Two concrete bridge deck specimens from the I-469 bridge over Feighner Road were heated for different time durations (40 - 80 min.) following the ISO-834 temperature-time curve. The deck specimens were cooled naturally after the specific heating durations. The temperature profiles through the depth of deck specimens were measured during heating and cooling. After testing, concrete samples were taken from the deck specimens for material analysis. Different types of material tests were conducted on samples taken from the undamaged and damaged deck specimens. The material test results were used to evaluate the effects of fire induced damage on the concrete microstructure, and to correlate the microstructure degradation with the through-depth temperature profiles of deck specimens.

From the experimental results, several critical parameters that can affected by fire temperature and duration were discussed: (i) through-depth temperature profiles of deck specimens, (ii) cracks on the exposed surface of deck specimens, (iii) color changes of deck specimens, (iv)

microstructure of heated concrete samples, (v) content of calcium hydroxide in fire damaged concrete samples at various depths. Based on the results from heating experiments and observations from material analysis, recommendations and guidance for evaluating concrete decks subjected to realistic fire scenarios are provided to assist bridge inspectors.

1. INTRODUCTION

1.1 Background

Although not very common, bridges with concrete components do occasionally get damaged by fire events. After the event, it is difficult for bridge inspectors to establish the intensity of the fire event, the concrete surface temperatures, and the associated damage (at material and structural level) due to fire. Research-based guidance is needed for bridge inspectors to assess and evaluate the material and structural integrity of concrete components exposed to fire events. This guidance should address the extent of damage, the potential for repair, and the need for partial or complete replacement of concrete components subjected to fire events. The focus of the study presented in this thesis is on the post-fire assessment of concrete in bridge deck components, on providing guidance for evaluating material and structural integrity after a significant fire event.

1.2 Project Objectives

The main objectives of this project were to:

- Conduct a literature review of the current state-of-knowledge regarding the assessment of concrete bridge components damaged by a fire event;

- Evaluate the effects of fire induced damage on concrete bridge deck elements, including color change, cracking, and spalling;

- Measure the surface temperature and through-depth temperature profiles of concrete deck members exposed to heating with temperature curves obtained from ISO-834 fire temperature-time curve;

- Evaluate the effects of fire induced damage on the concrete microstructure, and to correlate the microstructure degradation with the through-depth temperature profiles of deck specimens;

- Develop recommendations and guidance for bridge inspectors to assess the quality of concrete bridge deck components subjected to a fire event.

1.3   Summary of the Thesis

Chapter 2 presents a review of existing literature on the effects of elevated temperature and fire-induced damage on concrete bridge components. Case studies of several concrete bridge exposed to fire are discussed.

Chapter 3 introduces the experimental program for this research. This chapter describes the test setup and instrumentation for heating tests conducted on concrete deck specimens obtained from a decommissioned bridge in Indiana. The chapter also discusses the sample preparation and procedures for conducting material tests on cores taken from the heated and unheated concrete decks.

Chapter 4 presents the test results from the heating experiments performed on concrete deck specimens and the results of material tests conducted on the concrete core samples.

Chapter 5 concludes with providing recommendations for evaluating the effects of fire on the material and structural integrity of concrete bridge deck components.

2. LITERATURE REVIEW

2.1 Case Study – Prestressed Bridge under Fire

In 2002, a railroad tanker collided on a prestressed girder bridge and caused a fire under the bridge, and the incident was inspected by the Washington State Department of Transportation (WSDOT), and reported by Stoddard (2004). About 30,000 gallons of methanol was consumed during the fire. The flame temperature of the fire was estimated to be around 3000°F (1649°C). This study also showed the comparison of temperature vs. time curves between furnace test according to ASTM E119 and methanol tanker fire, as shown in Figure 2-1, which indicates that although methanol fire can cause higher temperature compared to furnace heating, the duration of high temperature period is shorter than the duration of elevated temperature period in the furnace tests. According to Stoddard (2004), it is likely that the temperature of the bottom of the girders reached to almost 2700°F (1482°C) after only 30 minutes.
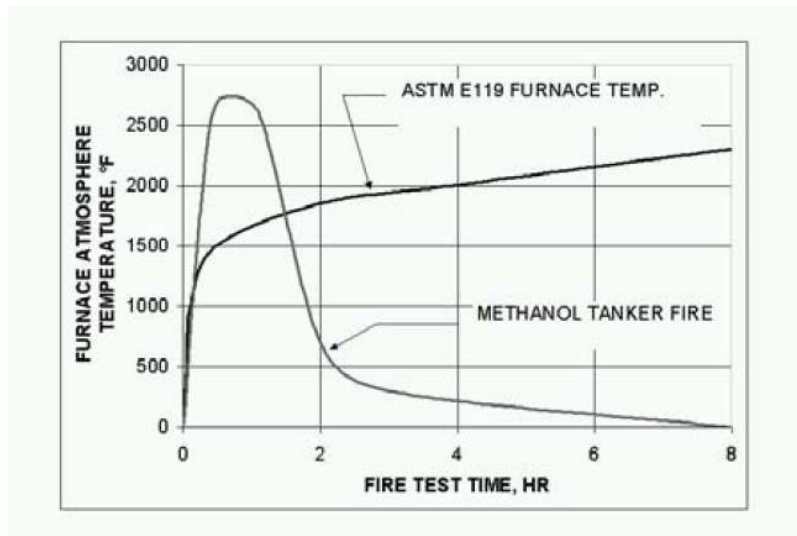
Figure 2-1. Temperature vs. Time for ASTM E119 Furnace and Methanol Tanker Fire (Stoddard, 2014)

Inspections and evaluations have been conducted by WSDOT, including visual inspections, prestressed steel evaluations, concrete hardness tests, and core sample evaluations. According to the results from inspections and evaluations, the surface temperature on the soffit of the prestressed girders was estimated to be around 1700°F (927°C), with the internal temperature in the bottom flanges and webs ranging from 500°F to 1100°F (260°C to 593°C). The damage of the concrete in the girders and columns was caused by the rapid heating and cooling rates. The outer part of concrete spalled and fell off, but the compressive strengths still exceeded 9000 psi, which indicates the residual strengths for remaining concrete are still adequate.

An accident involving truck fire in Connecticut was reported by Graybeal (2007). In 2005, a gasoline tanker truck overturned and exploded causing significant damage to a box-beam bridge in southwestern Connecticut. About 8,000 gallons of burning fuel flowed over the bridge, and the temperature of the truck could have been over 4472°F (2467°C). A series of tests were carried out on the beams removed from the bridge after the fire in order to study their post-fire residual capacities. Four beams were selected from different areas in the bridge and used to conduct flexural capacity tests. The results from those four beams showed that even the most damaged beam had the ultimate flexural capacity that was more than 10% higher than the analytically determined flexural capacity of the beam not damaged by the fire. This indicates that the remaining flexural capacity of beams damaged by fire was still adequate. However, the long-term viability of the fire-damaged beams was more questionable, as the bottom flange concrete and strands may have experienced accelerated deterioration which can cause a long-term decrease in the flexural capacity of the beams.

A fire that damaged Chase Street bridge in Indiana was evaluated by Ashraf and Olek (2016). In 2015, the truck fire under the Chase street overpass near Gary, Indiana caused damage

to several girders of the bridge, due to the collision of a semi-truck with the bridge in Indiana. An investigation was performed by Ashraf and Olek (2016) on the concrete samples extracted from the girders. The evaluation of concrete includes visual assessment of general conditions of concrete, detailed examination of the microstructure using Scanning Electron Microscopy (SEM) and Energy Dispersive Spectroscopy (EDS) techniques, and determination of change in the amount of calcium hydroxide (CH) in hydrated cement paste using Thermogravimetric Analysis (TGA) technique. Based on the results of investigations, cracking, debonding of aggregate, and increased micro porosity could be found near the surface of the concrete sample, which indicated that CH and calcium – silicate – hydrate (C-S-H) matrix were partially or fully decomposed and that the temperature around this area could be in the range of 752°F to 1112°F (400°C to 600°C), and this range of temperature indicated that the concrete could lose as much as 60% of its original strength. With increase of the distance from the surface towards the interior of the sample, it seems that the inner region of the sample also had some levels of microstructural cracking that can be due to the decomposition of C-S-H, which suggested that the inner region exposed to the fire temperature in the range of 212°F to 572°F (100°C to 300°C). The loss of the evaporable water caused the reduction of stiffness of C-S-H when temperature reaches to around 302°F (150°C), 60% of its stiffness was estimated to be lost based on the corresponding temperature range, according to Ashraf et al (2016).

As a conclusion, from these case studies, it is very important to provide inspection instructions to evaluate the damage of the bridge due to fire in order to observe and identify concrete damage zones immediately after a fire. Visual color mapping needs to validate and correlate with the concrete properties so that bridge inspectors can evaluate the concrete damage

zones and estimate the fire temperature through depth and residual strength of concrete based on visual inspections.

2.2   Concrete Exposed to High Temperature

Concrete properties can be largely affected by high temperature. This section summarized the previous studies on concrete exposed to high temperature. At elevated temperature, not only the reduction in material properties but also the visual change, such as surface color, cracks, spalling, and microstructure degradation can be observed in concrete. Details will be discussed in the following subsections.

2.2.1 Microstructure of Concrete

Increase in temperature can cause the change in the microstructures of both cement paste and aggregate in the concrete. According to Hager (2013), with temperature increasing, cement paste results in losing moisture, starting with free water, followed by capillary water, then physically bound water, and eventually water chemically bound with cement hydrates, which affects the mechanical properties of cement paste. For calcium hydroxide (CH), which is normally found in the transition zones between aggregate and cement paste, it starts to dehydrate at 752°F (400 °C). The physical and chemical change of aggregate due to temperature is governed by the main minerals of the aggregate. For example, quartz in fine aggregate changes phase from α to β at 1065°F (574 °C), which causes volume increase and eventually cracks through thickness of concrete. For carbonates in coarse aggregate (e.g. limestone and dolomite), it decomposes into lime and gas at around 1292°F (700°C). The gas can cause additional cracking and spalling. A summary table with the list of changes in concrete during heating is summarized by Hager (2013) and shown in Figure 2-2.

Temperature range	Changes
20–200°C	slow capillary water loss and reduction in cohesive forces as water expands; 80–150°C ettringite dehydration; C-S-H gel dehydration; 150–170°C gypsum decomposition ($CaSO_4 \cdot 2H_2O$); physically bound water loss;
300–400°C	approx. 350°C break up of some siliceous aggregates (flint); 374°C critical temperature of water;
400–500°C	460–540°C portlandite decomposition $Ca(OH)_2 \rightarrow CaO + H_2O$;
500–600°C	573°C quartz phase change $\beta - \alpha$ in aggregates and sands;
600–800°C	second phase of the C-S-H decomposition, formation of β-C_2S;
800–1000°C	840°C dolomite decomposition; 930–960°C calcite decomposition $CaCO_3 \rightarrow CaO + CO_2$, carbon dioxide release; ceramic binding initiation which replaces hydraulic bonds;
1000–1200°C	1050°C basalt melting;
1300°C	total decomposition of concrete, melting.

Figure 2-2. The List of Changes Taking Place in Concrete during Heating (Hager, 2013)

2.2.2 Properties of Concrete

According to Griffin and Beavis (1992), concrete exposed to high temperature will experience reduction of its compressive strength, modulus of elasticity, and stiffness. Degradation of concrete properties depends on the type of aggregate. Aggregates are mainly divided into two types: carbonate aggregates and siliceous aggregates. Carbonate aggregates include limestone, limerock, and dolomite, all of which contain calcium and/or magnesium carbonate. The carbonate aggregate will undergo a thermal decomposition in the temperature range of about 1110°F to 1470°F (600°C to 800°C). This decomposition releases carbon dioxide (CO2) which can cause considerable volume contraction and cracking of concrete, according Ingham (2009).

Siliceous aggregates include silicon dioxide. For siliceous aggregates, they do not undergo any chemical changes within the temperature range of fire tests. Figure 2-3 also shows the change of compressive strength at elevated temperature for concrete using different types of aggregate. As shown in Figure 2-3, the strength of concrete with all types of aggregates starts to reduce when temperature reaches to about 800 °F (about 400 °C), which is also the temperature that calcium hydroxide (CH) in concrete decomposes.
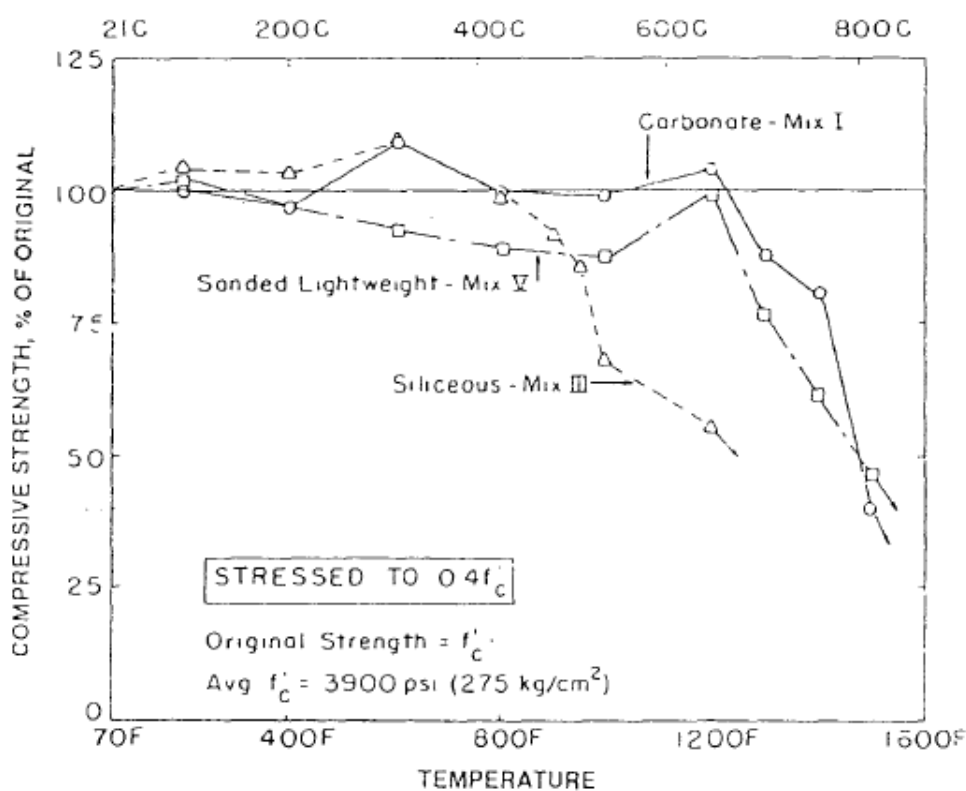
Figure 2-3. Compressive Strength of Concrete at High Temperatures (Griffin and Beavis, 1992)

When the temperature is at 410°F (210 °C), modulus of elasticity decreases to 70% of original value. When the temperature is at 788°F (420 °C), modulus of elasticity decreases to 50% of original value. When the temperature is at 1166°F (630 °C), modulus of elasticity decreases to 30% of original value.

Griffin and Beavis (1992) also explained that the thermal stresses become higher than the compressive stresses when bridge deck is exposed to fire on one side. Also, rising temperature can cause further hydration of the cement and eventually a degradation in bond.

2.2.3 Color Change

According to Lee, Choi, and Hong (2012), high temperature can cause a change in color and decrease in residual compressive strength of concrete. The color of concrete changes to red at 572°F to 1112°F (300 °C to 600 °C), whitish grey at 1112°F to 1652°F (600 °C to 900 °C), and buff at 1652°F to 1832°F (900 °C to 1000 °C). According to Griffin and Beavis (1992), color changes in concrete can also be affected by the type of aggregate used in the concrete. The color change is more evident in siliceous aggregate, compared with other types of aggregate. Griffin and Beavis (1992) also mentioned that a change in hydration states of iron oxides happens due to iron inside the aggregate if concrete turns into pink color.

2.2.4 Cracks and Spalling

Lee, Choi, and Hong (2012) stated that high temperature can also cause some visual changes, such as cracks, to concrete. When temperature is below 1112°F (600 °C), no crack or other changes is found. When temperature is higher than 1292°F (700 °C), cracks from 0.2 mm to 1.0 mm are observed. According to Griffin and Beavis (1992), expansion in concrete can be caused by increase in temperature, but the temperature increase can also lead to the shrinkage of the hardened concrete paste, which eventually can cause micro cracks during cooling process.

Griffin and Beavis (1992) mentioned that spalling can be caused by one-side heating on bridge deck, when temperature is increased rapidly on one side while the other side is still cool. Also, increase in temperature can lead entrapped water to vaporize and result in spalling.

2.3   Strands Exposed to High Temperature

Based on previous works related to the high temperature, residual strength and related behaviors of prestressing strands is summarized in this section. As shown in many experiments, after the fire, the strand may not remain its ultimate tensile strength even if it may still seem functional. Considering the safety of structures, the performance of the structure should be examined not only during the fire but also after the fire when the structure has already been cooled down. Several tests conducted by different research institutions with various perspectives and approaches have been studied and summarized as below.

2.3.1 Residual Strength

With heating the strand for a long period of time to various peak temperatures then cooling it down, residual ultimate strength of the strand decreases starting at when the maximum heating temperature exceeds 572°F (300 °C). According to Moore et al. (2008), the reduction of the residual strength starts increasing significantly when the temperature reaches to 752°F (400 °C), and at 1292°F (700 °C), only 38% of ultimate tensile strength remains. Residual strength of the strands also depends on the time that strands were soaked in the furnace. Strands soaked at certain one temperature with shorter period has better performance on their residual strength. However, variation of cooling methods of strands will not provide much different results for the residual strength.

2.3.2 Relaxation

Similarly, stress relaxation occurs on the strands due to the heating, and the loss becomes irrecoverable after the maximum temperature reaches to 752°F (400 °C), according to MacLean et al. (2008), The relaxation behavior is also affected by the maximum temperature applied to the strands. Higher temperature will produce much more stress relaxation losses. However, MacLean

et al (2008). also stated that relaxation is not affected by the time duration. As long as the temperature exceeds 752°F (400°C), even for a short period of exposure, the relaxation losses are still significant and irrecoverable.

2.3.3 Yield Strength and Modulus of Elasticity

Yield strength of strands can also be affected by the maximum temperature to which strands have been exposed. With exposure to the higher temperature, strands can become more brittle and result in fracturing immediately after yielding or even before yielding. Also, the modulus of elasticity of the strands will not change much due to the high temperature applied to the strands.

2.4   Previous Research

Several heating tests from other researchers are briefly introduced in this section. Both heating tests were conducted using furnace as main heating equipment to simulate real fire scenario. Temperature results from this project will be compared with ones from other research projects in future chapters to verify the accuracy and of the heating method and test result.

2.4.1 Zheng (2008)

Zheng (2008) has conducted a series of fire experiments to study the mechanical behavior of prestressed concrete simply supported slabs subjected to fire. A furnace with dimension of 3 m by 4 m was used as heating equipment for the tests. The overview of the furnace used in Zheng's experiments is shown in Figure 2-4.
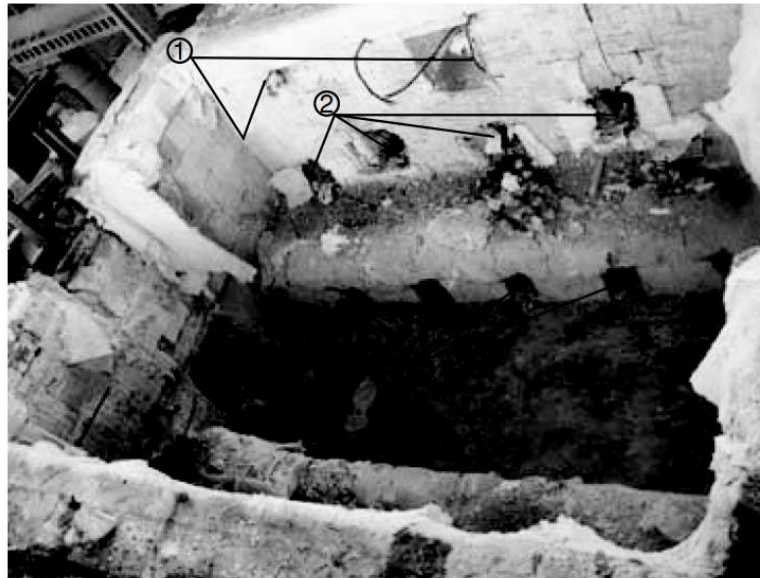
① fuel injection ② Thermocouples monitoring temperature
of furnace ③ exhaust system

Figure 2-4. Overview of the Furnace (Zheng, 2008)

The results from Zheng (2008) is shown in Figure 2-5. From the figure, it is found that the tested temperature curve from thermocouples that were located near the exposed slab surfaces (short dashed line) was slightly lower than ISO 834 standard fire temperature (long dashed line), during the furnace test. This tested temperature measurements will be compared with the temperature measurements from this project tests in the future chapters.
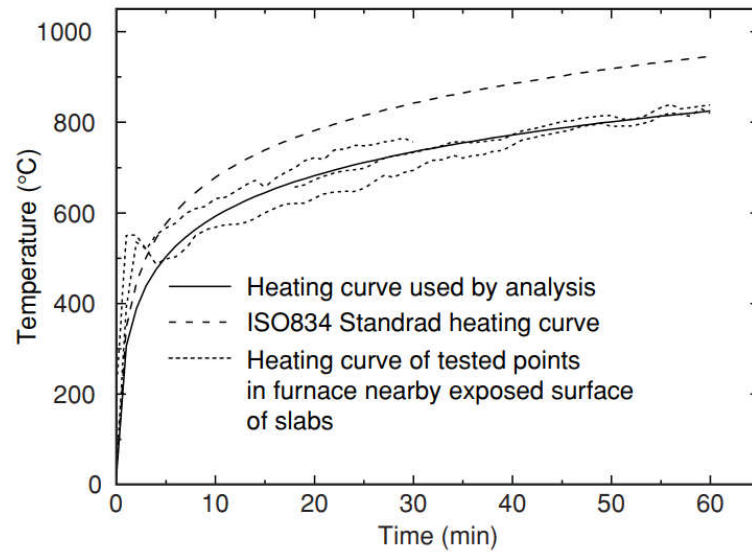
Figure 2-5. Surface Temperature Compared with ISO 834 Standard Heating Curve (Zheng,

2008)

2.4.2 Hou (2014)

Hou (2014) has also conducted a series of fire experiments using furnace as heating

equipment. The heating chamber of the furnace with dimension of 3 m by 4 m by 2.46 m was used

as heating equipment, and eight oil burners are located inside the furnace in order to provide

thermal energy. Thermocouples were distributed throughout the chamber to measure furnace

temperature during the test. Figure 2-6 shows the comparison of temperature measurement from

thermocouples attached at the furnace with ISO 834 standard fire curve. The temperature results

from the furnace test verified that using furnace to simulate fire event can provide very similar air

temperature compared to standard fire temperature curve. The surface temperature results from

Hou (2014) will also be discussed and compared with the experimental results from this project in

the future chapters.
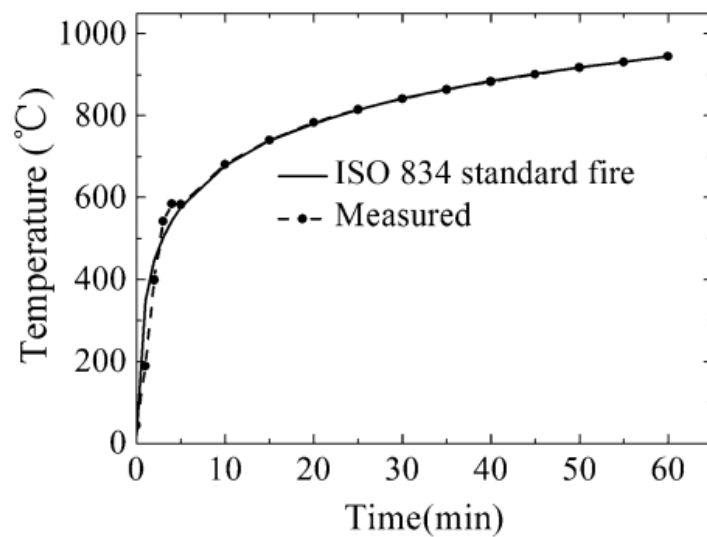
Figure 2-6. Measured Temperature in the Furnace during Fire Tests (Hou, 2014)

3. EXPERIMENTAL PROGRAM FOR CONCRETE DECK TESTS

3.1 Introduction

This chapter presents the design and setup of experimental investigations conducted on two concrete deck specimens under different heating periods. All concrete deck specimens were taken from I-469 bridge over Feighner Road. One-side heating tests were conducted using high-temperature ceramic heaters to evaluate the thermal and mechanical behavior of the specimen and measure the temperature profiles through depth. Material tests were also conducted on samples taken from concrete cores from the specimen after heating. These material tests were conducted to evaluate concrete microstructure degradation. This chapter is subdivided into following sections:

- Section 3.2 provides an overview of test program.

- Section 3.3 presents the details and preparation of the test specimens, including the preliminary test conducted prior to the heating test.

- Section 3.4 describes the heating system setup and the instrumentation layout for the heating experiments.

- Section 3.5 discusses the testing procedure used for heating the deck specimens.

- Section 3.6 describes the testing procedure used for the material tests.

3.2 Overview of Test Program

The objective of this test series was to evaluate the thermal and mechanical behavior of the concrete of the deck specimens, measure the temperature profiles through the depth of concrete, and evaluate the microstructure degradation by examination of cored samples.

Two concrete deck specimens were tested for 40 minutes and 80 minutes of heating following the ISO-834 heating time-temperature curve. All deck specimens have the dimension of 48 in. by 48 in. with thickness of 8 in. The deck specimen was supported on rollers with 3 ft distance in between to allow free expansion in horizontal direction and provide supports in vertical direction. The rollers were 6 in. away from each end of the deck. The roller support system was placed on two 2 ft high concrete blocks to allow the instrumentation to be placed under the deck. The test setup is shown in Figure 3-1.
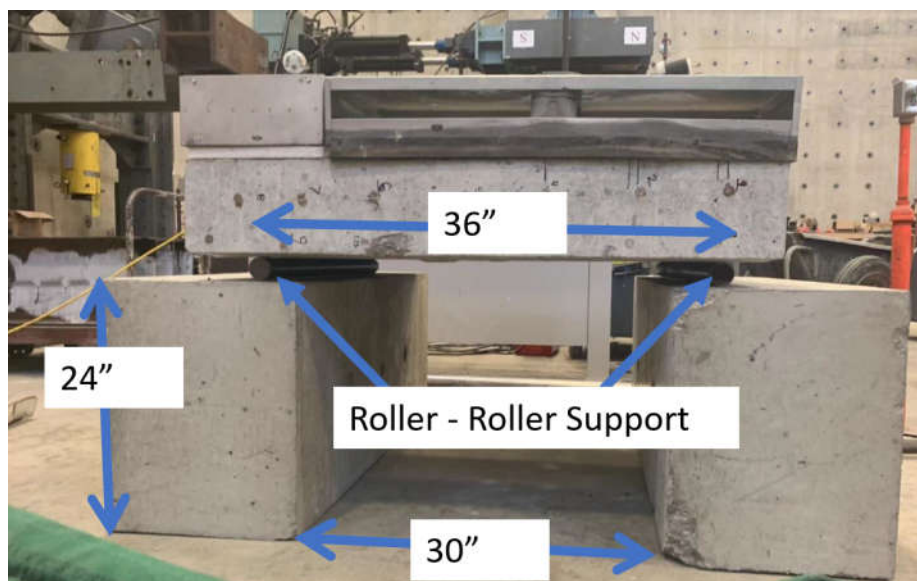
Figure 3-1. Test Setup for Heating Experiment

3.3   Test Details

3.3.1 Specimen Details

All test specimens were collected from I-469 bridge over Feighner Road, a bridge located near Fort Wayne, Indiana, whose service history was more than 30 years. Deck sections were selected from the green area shown in Figure 3-2. The deck sections were then transported to Bowen Laboratory for testing. As shown in Figure 3-3, two pieces of deck sections with

dimensions of 4 ft by 10 ft by 8 in. were originally cut from the bridge. A coat of epoxy was on

top of the deck section when the deck was cut from I-469 over Feighner Road.
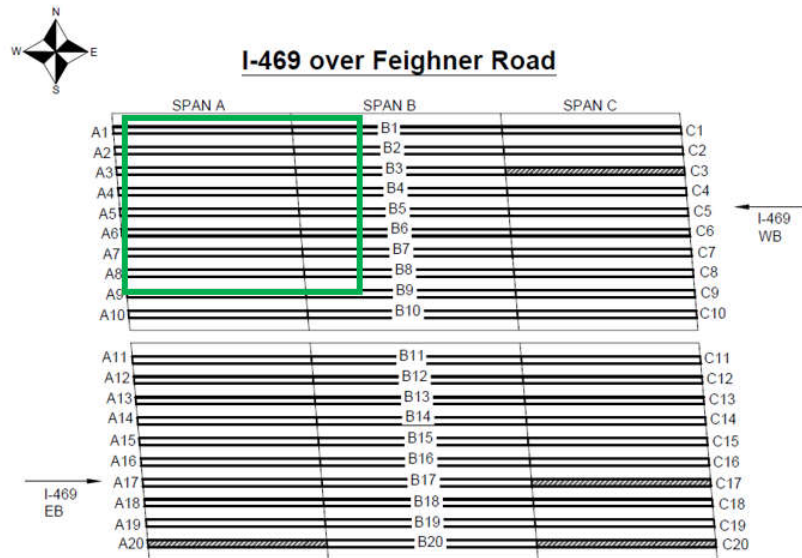
Figure 3-2. Plan View of I-469 over Feighner Road

Figure 3-3. Original Deck Sections Removed from I-469

After deck sections were transported to Bowen Laboratory, each section was cut into two

deck specimens for testing, as shown in Figure 3-4. In total, four deck specimens with dimensions

of 48 in. by 48 in. were cut from the original sections.

Figure 3-4. Deck Specimens Cut from the Original Deck Sections

All deck specimens were placed under the halogen lamp drying system for two weeks in order to evaporate excessive surface moisture from the specimens. The halogen lamps drying system were located about 6 in. above the deck specimens to ensure that the concrete surface temperature does not exceed around 140°F (60°C); such temperature is high enough to evaporate surface moisture and dry out the specimen, but it will not remove the chemically bonded water from various hydrated phases present in hardened concrete. The halogen lamps drying system is shown in Figure 3-5.
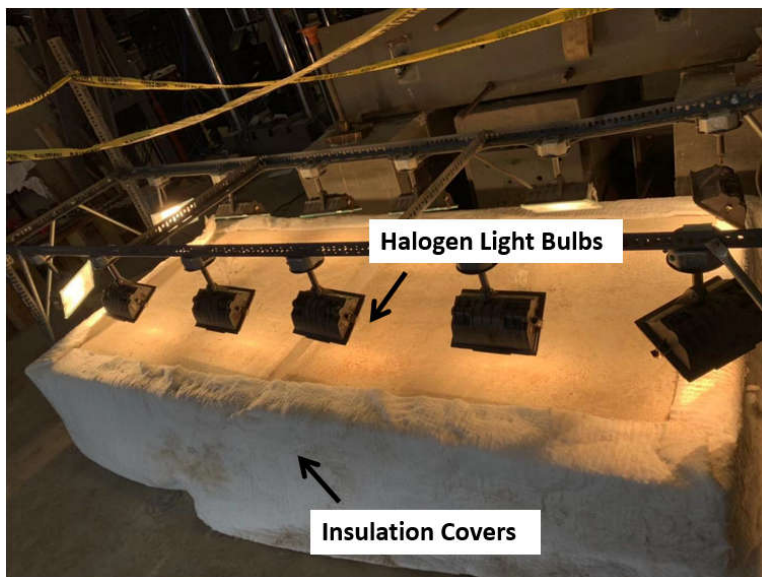
Figure 3-5. Halogen Lamp System

3.3.2 Preliminary Heating Test

A preliminary test was prepared and conducted in order to validate the installation method of thermocouple trees for the deck specimen and to verify that the testing method was representative to the standard fire test.

For the preliminary test, small beams with cross-section dimension of 6 in. by 6 in. and length of 22 in. were cast for testing. The specimen for the preliminary test will be referred as small beam in future sections. One thermocouple tree was installed before casting and another one was installed after casting in order to compare the temperature profiles between two sets of thermocouples. Temperature results from both sets of thermocouple trees were compared with temperature results obtained from other references in the literature to validate the accuracy of the instrumentation setup. The thermocouple trees measured the temperature at 1 in., 1.5 in., and 2 in. depth in the small beam respectively.

During the casting process, one set (Set A) of thermocouple trees was installed before casting, as shown in Figure 3-6. After the beam had been cured for a week, a 2 in. diameter hole was drilled to insert another set (Set B) of thermocouples, as shown in Figure 3-7 and Figure 3-8.
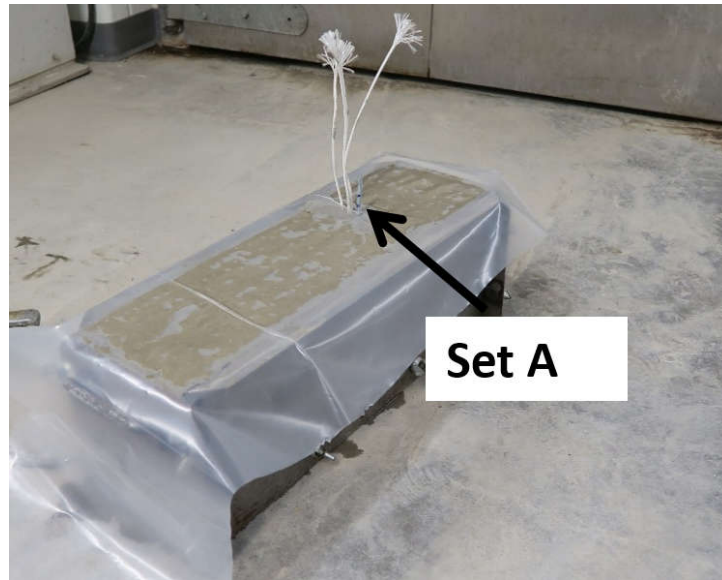
Figure 3-6. Small Beam during Casting Process

Figure 3-7. Drilling Process after the Curing Process of Small Beam
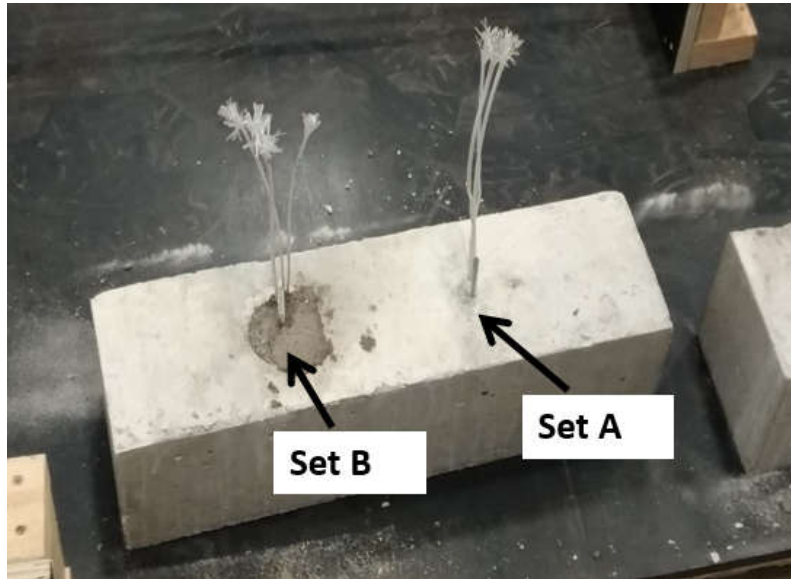
Figure 3-8. Installation of Thermocouple Tree after Casting

Once both sets of thermocouple trees were installed, packaged concrete mix was filled in the hole and cured for another week. Then the small beam was oven dried for one week with the heating temperature controlled by the oven, as shown in Figure 3-9. The oven temperature was set to 140°F (60°C) in order to evaporate the excessive surface moisture but not to break the chemically bonded water inside concrete inside the concrete. Two surface thermocouples were also installed for measuring the surface temperature.

Figure 3-9. Oven-Dry Process for Small Beam

Once the small beam was placed in the oven for a week, it was ready for heating experiment. The experiment was set up as shown in Figure 3-10. Insulation blocks were put on top of the small beam to avoid heater from coming into direct contact with concrete surface.
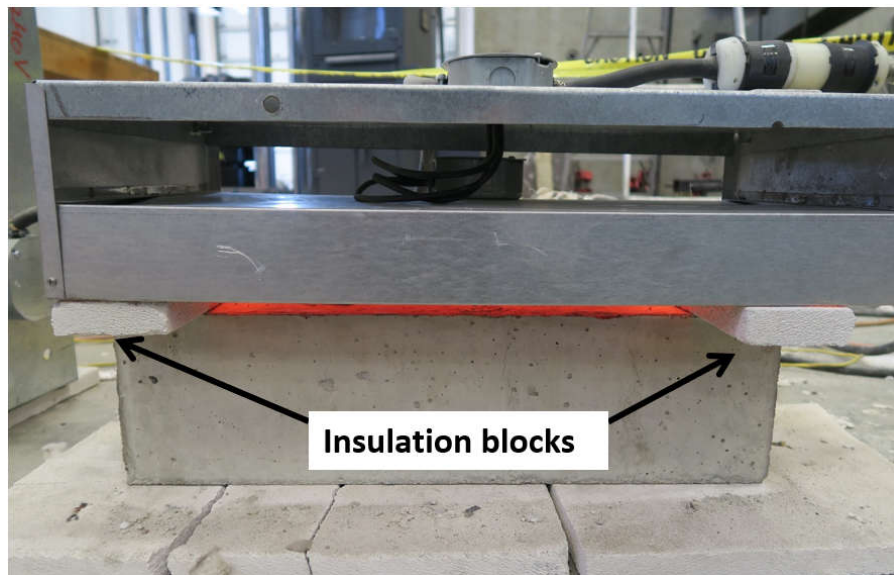
Figure 3-10. Preliminary Test Setup

The small beam was heated for 100 minutes. The surface temperature reached approximately 1300°F (704°C). results for preliminary test will be presented in the next chapter. Surface temperature was also monitored using handheld non-contact temperature indicator during experiment, as shown in Figure 3-11.

Figure 3-11. Surface Temperature Verification by Handheld Temperature Indicator

3.4   Deck Heating Test Setup and Instrumentation

3.4.1 Heating System Setup

As mentioned earlier, the deck specimens were taken from the bridge deck of I-469 bridge over Feighner Road. The top surfaces of the bridge decks were covered with overlay materials, which were left intact. The deck specimens were oriented such that the surface with overlay materials (top surface of the bridge deck) was on the bottom of the setup. In the setup, the deck specimens were subjected to one sided heating from the top, which was the bottom surface of the bridge deck. In a fire event, the bottom surface of the bridge deck is most commonly exposed to heating / fire, so the heating location in the setup was appropriate.

High-temperature ceramic-fiber radiant heaters were used to heat the deck specimens. Five ceramic heaters were placed above the deck, including three 36 in. by 16 in. heaters (Heater 1 to Heater 3) and two 24 in. by 12 in. heaters (Heater 4 and Heater 5), as shown in Figure 3-12. The ceramic-fiber radiant heaters were produced by Watlow Electric Manufacturing Company.
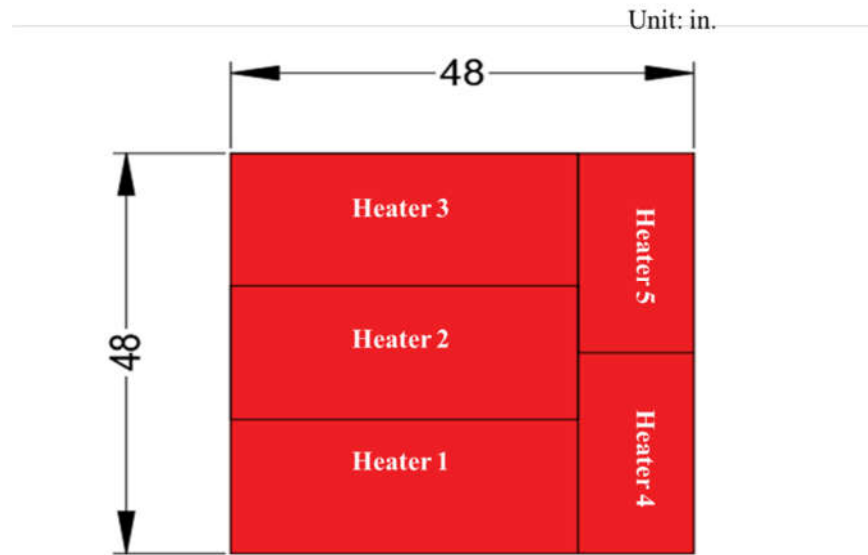
Figure 3-12. Layout of Ceramic Heaters for Heating System

Ceramic insulation cloth was placed in the gaps between heaters and at the edge of heaters. It can prevent heat loss during the test and avoid sensors from catching fire. Ceramic insulation blocks were also placed between the heater surface and the deck specimen so that heaters were not in contact with the specimen.

SpecView was used to individually control the heater temperature and record the surface temperature measured by the surface thermocouple readings through the control panel. SpecView was also used to record the temperature profile for the thermocouple tree embedded inside the deck specimen.

3.4.2 Thermocouples

Thermocouples were used to measure the temperature history at specific locations throughout the test. Type-K thermocouples were used, which are capable of measuring temperature up to 2600°F (1427°C). Thermocouples were placed at exposed surface of concrete to provide the temperature results at various locations during the test. One thermocouple tree was embedded at the center of the specimen to record the temperature through the depth of deck.

3.4.2.1 Surface Thermocouples

In order to provide the temperature measurements throughout the surface area, thermocouples were placed at exposed surfaces of the deck at locations that are 1 ft away from the edge, at the center of the deck specimen, at the center of the heaters, and at the gaps between each heater, respectively, as shown in Figure 3-13. In total, 14 surface thermocouples were installed on each deck specimen, with one redundant thermocouple under each heater to make sure that the heater temperatures could be controlled and recorded.
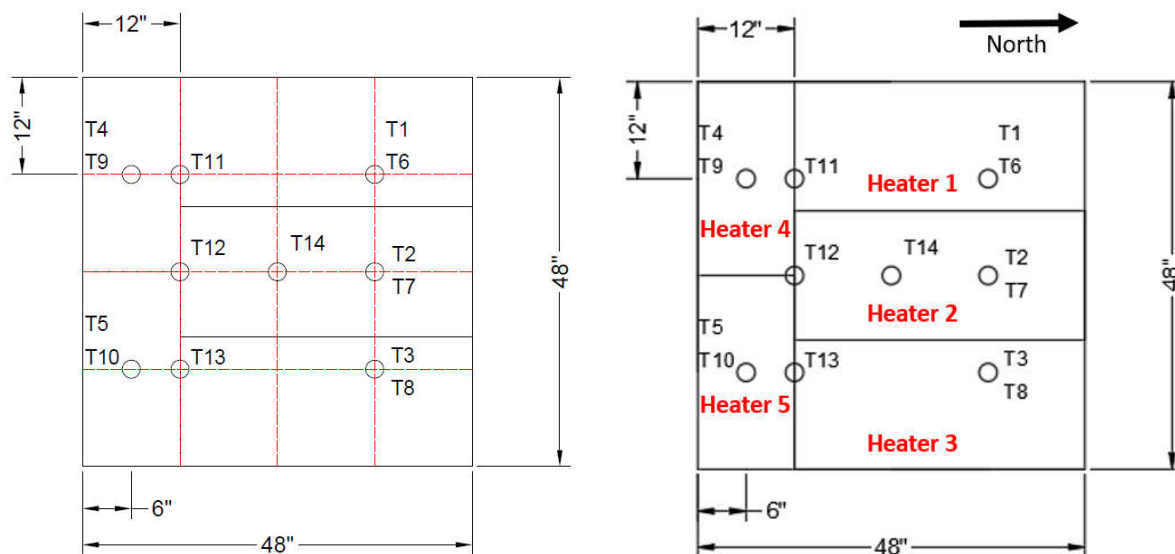
Figure 3-13. Layout of Surface Thermocouples

In order to allow thermocouples to measure surface temperature properly, a small hole with about 0.5 in. depth was drilled to place each surface thermocouple. The surface thermocouple was placed inside the hole with the measuring point attached on the surface of specimen. High temperature cement manufactured by Omega was used to fill the hole, fix the position of thermocouple, and prevent the thermocouple from direct contact with the air. An example of how the high temperature cement covers the surface thermocouple is shown in Figure 3-14.

Figure 3-14. Surface Thermocouple Covered by High Temperature Cement

3.4.2.2   Thermocouple Tree

To provide the thermal profile through the depth of the deck specimen, a thermocouple tree was embedded at the center of the deck. As shown in Figure 3-15, the thermocouple tree contains 9 thermocouples welded along a steel rod at various depth: 0.25 in., 0.5 in., 0.75 in., 1 in., 1.25 in., 1.5 in., 2 in., with one extra thermocouple welded at 3 in. electrically grounded to the data acquisition system.
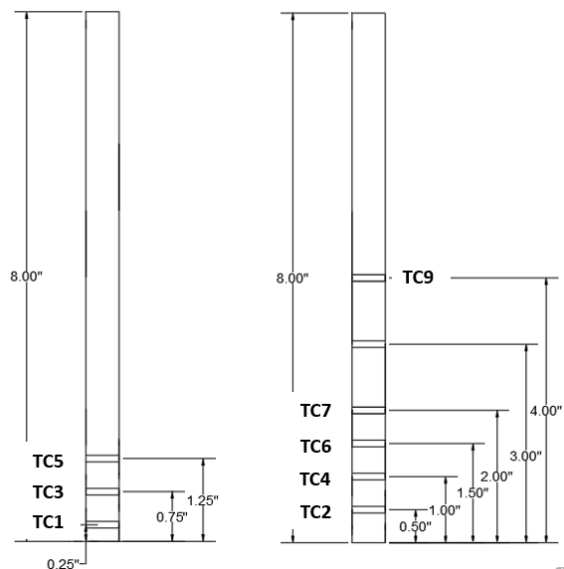
Figure 3-15. Thermocouple Tree Layout

Each thermocouple was welded to the steel rod with its junction extending out from the rod; the thermocouples were also covered by the high temperature cement for insulating the thermocouples. A 2-in. diameter hole was drilled around the center of deck specimen in order to place the thermocouple tree. After the thermocouple tree was positioned, the hole was filled by packaged concrete mix and cured for a week before the deck specimen was dried by halogen lamp system shown in Figure 3-5.

3.4.3 Displacement Transducers

Since the deck specimen was only heated but not loaded, the vertical displacements of the deck specimen were due to thermal expansion and estimated to be small. Displacement transducers (with 1-in. stroke) were used to measure the vertical displacement of the deck specimen.

In total, five displacement transducers were placed under the bottom face of the deck specimen, as shown in Figure 3-16. Four displacement transducers were located at quarter span, 12 in. from each edge, and one displacement transducer was at the center of the deck specimen.

Small S-shaped hooks were fixed to the bottom surface of the deck specimen using concrete screws. Displacement transducers were placed inside aluminum angle brackets and attached to a steel frame so that they were located at the destinated location for accurate measurement. Displacement transducers were in contact with the S-shaped hooks in order to measure the vertical displacements of the deck specimen. To protect the displacement transducers from the heat during the experiment, the displacement transducers were insulated by insulation block attached under the L brackets, as shown in Figure 3-17.
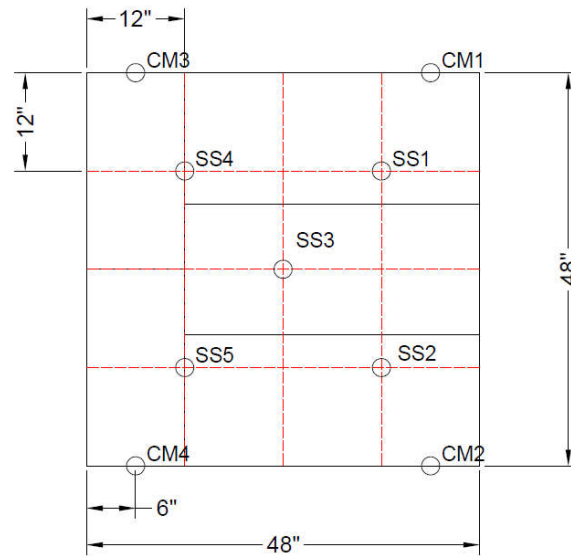
Figure 3-16. Displacement Transducers and Inclinometers Layout

Figure 3-17. Example of Protection of Displacement Transducers

3.5   Deck Heating Test Procedure

The summary of heating test procedure is shown below:

1. Before the test starts, set up the displacement transducers, inclinometers, and through depth thermocouples, and connect the instrumentation to the SpecView system. Apply small change of displacement, rotation, or temperature to the sensors to make sure that they can properly read the measurements.

2. Connect surface thermocouples to the control panel and record temperature measurements through SpecView. Place heaters on top of the deck specimen and put ceramic insulation blocks and fiberglass insulation between heaters and the deck specimen.

3. Turn on heaters through control panel and increase the temperature carefully to avoid the sharp increase in heater temperature within a short period of time.

4. Based on the observation from preliminary test, the heating protocol follows the ASTM standard fire test curve if the heaters are on and fully powered. Keep heaters for destined test duration, meanwhile keep track of the top and bottom surface temperature using handheld temperature indicator to make sure that the instrumentation readings are recorded properly.

5. When the test is finished, first turn off the control panel and then turn off heaters. Measure the surface temperature using handheld temperature indicator to compare with the readings from surface thermocouple measurements. Let the deck specimen cool down and record the temperature history during cooling curve.

6. After the deck specimen cools down, draw the observed cracks on the heating surface of the deck specimen to provide a map of cracks. Observe the deck specimen spalling for about two weeks. Collect the concrete powder from spalling for future material tests.

7. Drill a 2 in. by 4 in. core at the center of the deck specimen. The core will be used as the concrete sample for material tests.

3.6   Concrete Material Test Preparation and Procedures

3.6.1 Location of Tested Cores

All samples used in material analysis were collected from a core that was taken from the deck specimens before and after heating. The cored sample had the diameter of 2 in. and height of 8 in. As shown in Figure 3-18, the cores were removed from locations near the center of the specimen and close to the thermocouple tree so that the material analysis results can be correlated with the through-depth temperature profiles of the concrete.
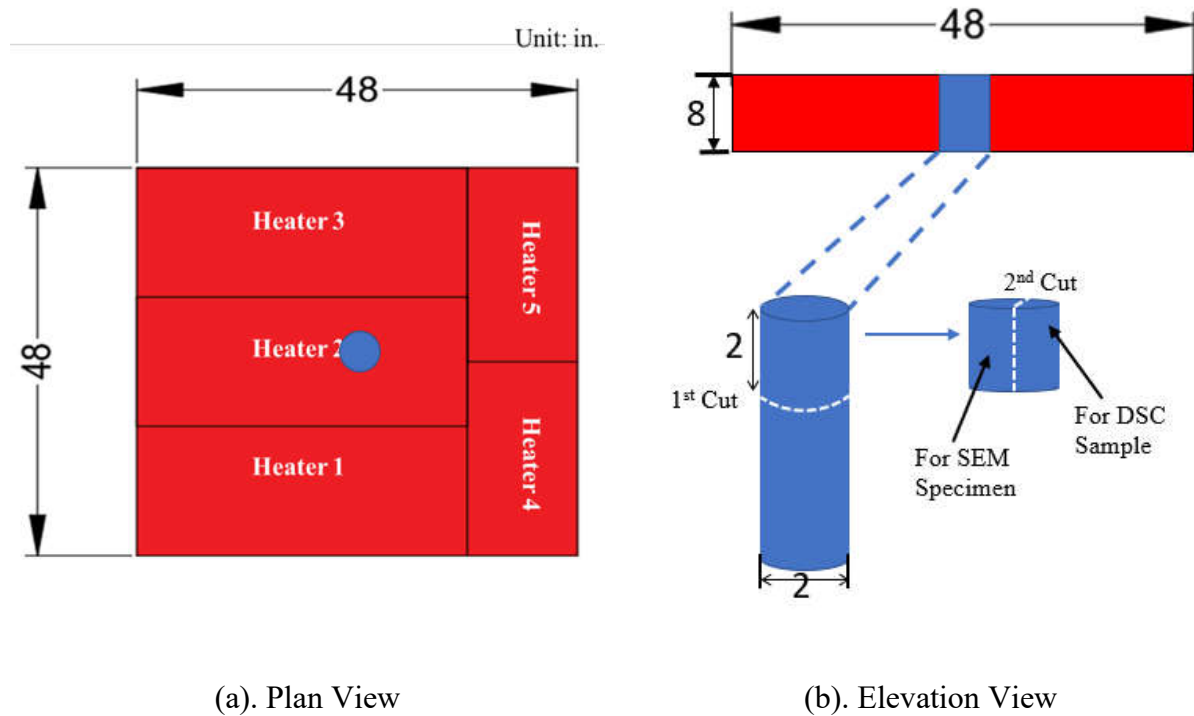
(a). Plan View   (b). Elevation View

Figure 3-18. Location of Material Analysis Samples at Deck Specimen

3.6.2 Preparation of SEM Samples

Scanning Electron Microscope (SEM) evaluation is a method of material analysis that provides information about the microstructure of concrete samples in terms of cracking, debonding of aggregates, and loss of phases by qualitative observations of the cross section of concrete specimens. The SEM was used in this research to compare the visual differences between concrete samples exposed to two heating tests (i.e. heated samples) with samples from original deck specimens (i.e. unheated samples).

The first step was cutting the cylinder cores, which were taken from the specimens before or after heating tests, to smaller pieces of samples. The cross-sectional area of SEM samples was selected from the exposed surface of core samples to about 1 in. depth. The cutting process is

shown in Figure 3-19. The sample cut from the core will be referred as the SEM specimen in the following sections.

Figure 3-19. Cutting Process of SEM Specimen Preparation

After the SEM specimen was cut into proper size for observation, it was oven dried under around 95°F (35°C) for three days to reduce the moisture inside the sample, as shown in Figure 3-20.

Figure 3-20. Oven Dry Process of SEM Specimen Preparation

After the SEM specimen was taken from the oven, the epoxy mounting was prepared for the SEM specimen, as shown in Figure 3-21. As shown in Figure 3-21, the solutions include: ERL – 4221, D.E.R. 736 Epoxy Resin, Nonenyl Succinic Anhydride, and Dimethylaminoethanol. The mixture was poured into the plastic molds, in which the SEM specimen was placed with the tested cross section facing top. To make sure no air was entrapped in the mixture, the SEM specimen was placed in the vacuum overnight, as shown in Figure 3-22. On the next day, the SEM specimen was taken out from the vacuum then put in the oven for 149°F (65°C) for approximately 8 hours to let the epoxy harden, as shown in Figure 3-23.

Figure 3-21. Solutions for Epoxy Preparation
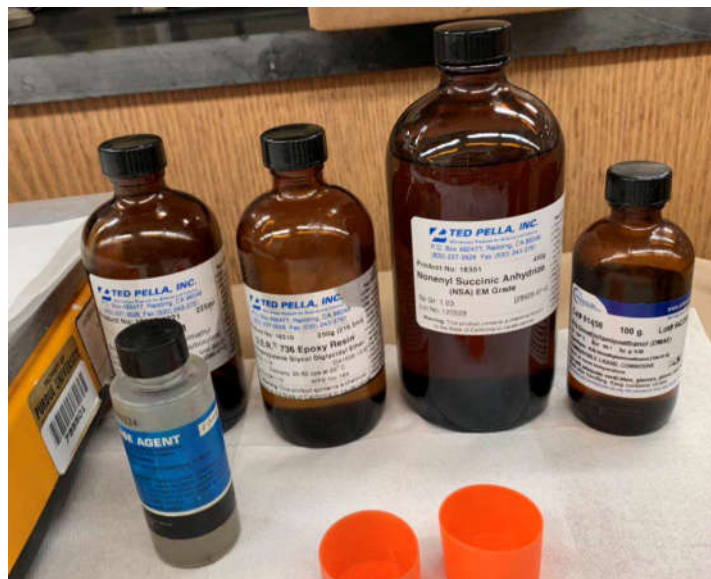

Figure 3-22. Vacuum Process for SEM Specimen Preparation

Figure 3-23. Oven Drying Process for SEM Specimen Preparation

When the epoxy in the SEM specimen hardened, the SEM specimen was moved away from the oven. The excessive epoxy layer at the top was removed using a diamond blade, as shown in Figure 3-24.
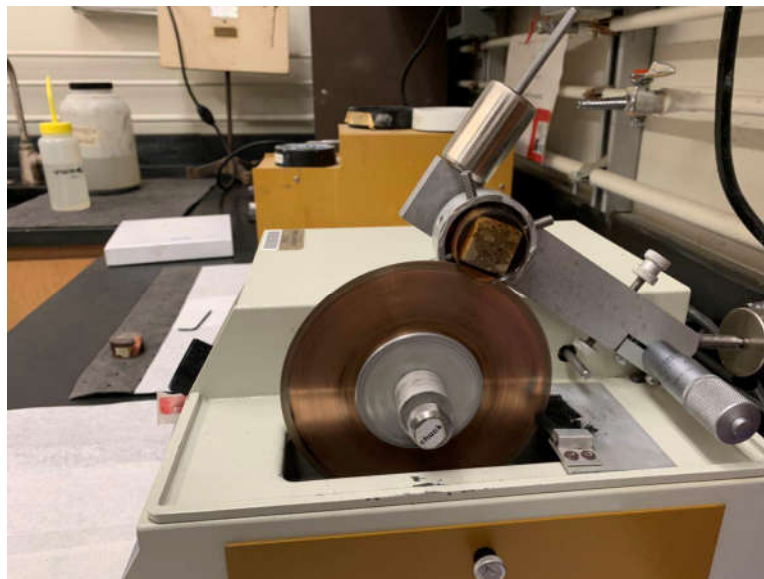

Figure 3-24. Sawing Process of Excessive Epoxy for SEM Specimen Preparation

Once the excessive epoxy layer of the SEM specimen was removed, the surface of concrete sample was exposed. Following this step, the surface of the SEM specimen needed to be lapped and polished to improve the dimensional accuracy and create a smooth surface of the SEM specimen for better results.

During the lapping process, the SEM specimen was placed on three lapping plates respectively with rotation at low speed to remove the subsurface damage on the specimen surface caused by sawing process. Three lapping plates are with the grit size of 45μm, 30μm, and 15μm respectively, and the plates were placed in the order from 45μm to 15μm. To produce smooth surface finish, one specimen needed to be polished for four directions, with 30 seconds for each direction, for twice for each lapping plate. The lapping process is shown in Figure 3-25.

Figure 3-25. Lapping Process for SEM Specimen Preparation

After the lapping process, the SEM specimen was polished using five different polish cloths and corresponding diamond pastes, with the size of 9μm, 6μm, 3μm, 1μm, and 0.25 μm, respectively. For each polish cloth, the specimen was placed in each direction for one minute with

four directions in total, and the polish cloth was placed in the order from 9μm to 0.25μm. After polishing process, the surface of SEM specimen was scratch-free, specular, and ready for observation under microscope. The polishing process is shown in Figure 3-26.
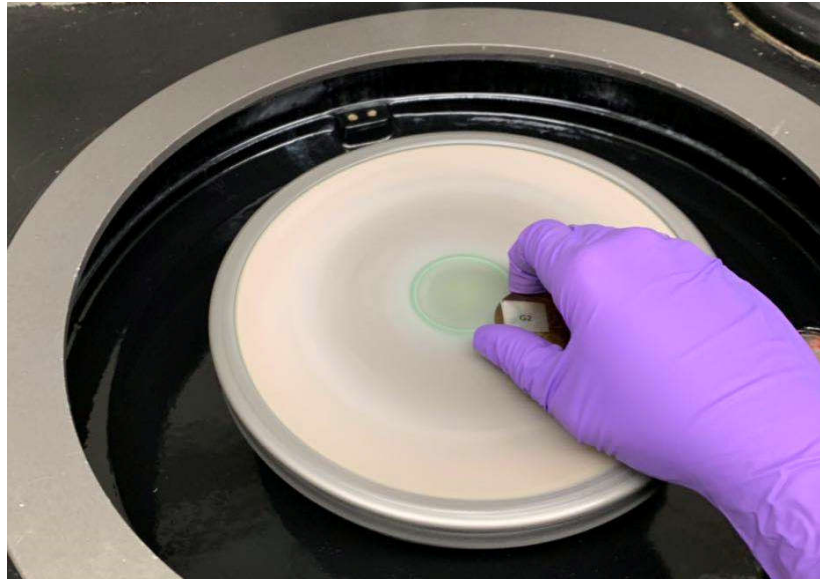

Figure 3-26. Polishing Process for SEM Specimen Preparation

3.6.3 Preparation of DSC Samples

Differential Scanning Calorimetry (DSC) is a method of material analysis that quantifies the content of various phases (i.e. calcium hydroxide for the purpose of this research) based on the peak area associated with energy required for the decomposition of the particular phase. Thus, DSC can be a good indicator of the impact of fire on certain characteristics of cement paste.

To prepare DSC samples, a small piece of concrete was achieved from the concrete core drilled from the deck specimen both before and after heating. Then the small piece of concrete specimen was grinded into powder using mortar and pestle while removing coarse aggregate during the grinding process, since DSC only needs to analyze the change of phases for the content inside the cement paste. The grinding process is shown in Figure 3-27.

Figure 3-27. Grinding Process for DSC Sample Preparation

After the concrete piece was grinded into powder, the powder was required to pass #200 sieve to make sure it is fine enough for DSC analysis. The grinding and sieving process were repeated until the volume of fine powder accumulated to enough amount for analysis. The fine powder will be referred as DSC sample in following sections. The sieving process is shown in Figure 3-28.

Figure 3-28. Sieving Process for DSC Sample Preparation

After DSC sample was prepared, about 10 mg to 18 mg of sample powder were measured from the DSC sample and transferred to an aluminum pan. The DSC sample was placed in the aluminum pan evenly so that the powder did not overflow the pan or inclined to one side of the pan. The weight of amount of DSC sample was measured and recorded for analysis use. An example of DSC sample inside the aluminum pan is shown in Figure 3-29.
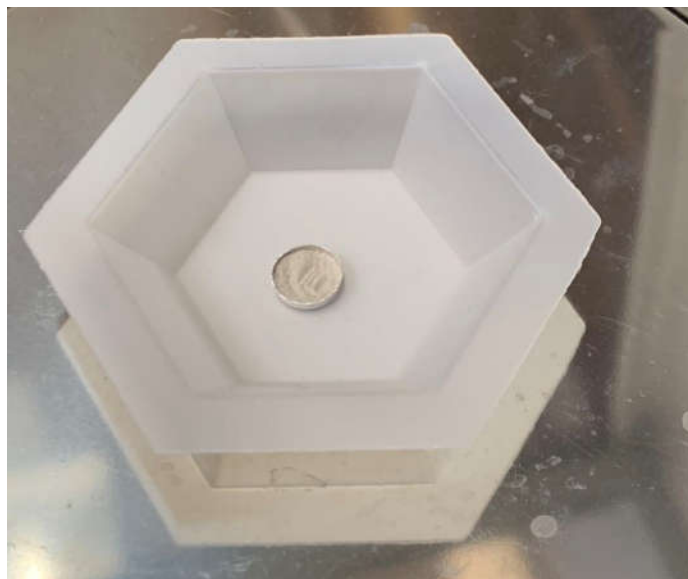
Figure 3-29. Example of DSC Sample Inside the Aluminum Pan

After the aluminum pan was filled with DSC sample, it was placed in the DSC instrument. The rate of DSC instrument was set to be 50°F/min (10°C/min) for the analysis. The DSC instrument is shown in Figure 3-30. Another empty aluminum pan was placed next to the DSC sample for comparison.
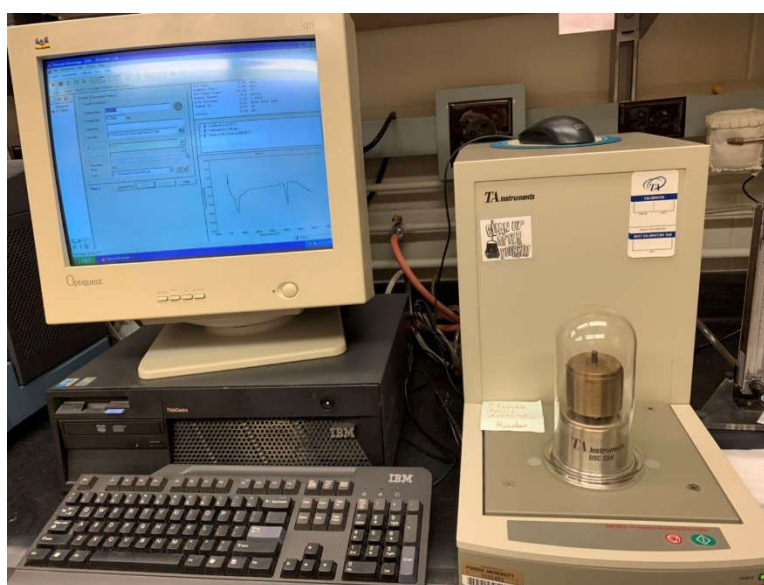

Figure 3-30. DSC Instrument

After the analysis was finished, results were exported from the computer and analyzed using TA instrument software. In order to understand the percent of calcium hydroxide (CH) in the DSC sample, a calibration curve of CH was also prepared. CH powders were mixed with fired kaolinite in various proportions (i.e. 0%, 10%, 20%, 50%, and 100% of CH). Fired kaolinite was used in mixing the calibration powder because the loss of water in fired kaolinite does not happen at the same time with CH. After the calibration curves were produced, peak area under the curve for each calibration curve was calculated using TA instrument software to represent the dissipated energy for the certain percentage of CH. Then content of CH can be calculated using the equation below:

$$\textbf{\textit{Content of CH (\%) = K x Peak Area (J/g)}}$$

where *K* is a constant that can be obtained from the calibration curves.

Using the equation above, the content of CH in the DSC sample can be then quantified and compared with the calibration curve.

4. EXPERIMENTAL RESULTS

4.1 Introduction

The chapter presents the experimental results from the heating tests and subsequent material tests. The chapter is subdivided into following sections:

- Section 4.2 discusses the results from heating tests conducted on concrete deck specimens, including preliminary test results for validating the experiment setup.

- Section 4.3 discusses the results from material tests conducted on concrete samples cored from the deck specimens, including both SEM and DSC analysis.

4.2 Heating Test Results

Two 48 in. by 48 in. deck specimens with a thickness of 9 in. were heated using high-temperature ceramic fiber radiant heaters on one side. One specimens was heated for 40 minutes, and one specimen was heated for 80 minutes. The results were used to evaluate the through-thickness temperature profiles of concrete. Material tests conducted on core samples taken from the heated and unheated specimens were used to evaluate microstructure degradation and correlate it with through-thickness temperatures.

4.2.1 Preliminary Heating Test

A preliminary heating test was conducted to verify the testing method, heating approach, and the surface and thermocouple tree installation method used in the laboratory. The results were verified by comparing the measured temperature histories from the test with those reported in the literature from standard fire tests. One small beam with cross-sectional dimension equal to 6 in. by 6 in. and length equal to 22 in. was cast and tested. One thermocouple tree (Set A) was installed

prior to casting, and another set (Set B) was installed after casting. The beam was over dried after installing the second set (B) of thermocouples. In this way, the temperature profiles measured and reported by the two sets of thermocouple trees (one placed before casting, and another installed after casting) could be compared. Both sets of thermocouple trees measured the temperature at 1 in., 1.5 in., and 2 in. distance from the heated surface. Two thermocouples were also installed to measure the surface temperatures during heating.

Figure 4-1 shows the temperature histories measured by both sets (A and B) of thermocouple trees in the small beam specimen at corresponding depths. It is evident that the temperature histories for Set A and Set B are very similar and comparable. Thus, the through depth temperatures can be measured accurately using thermocouple trees that installed either before or after casting.
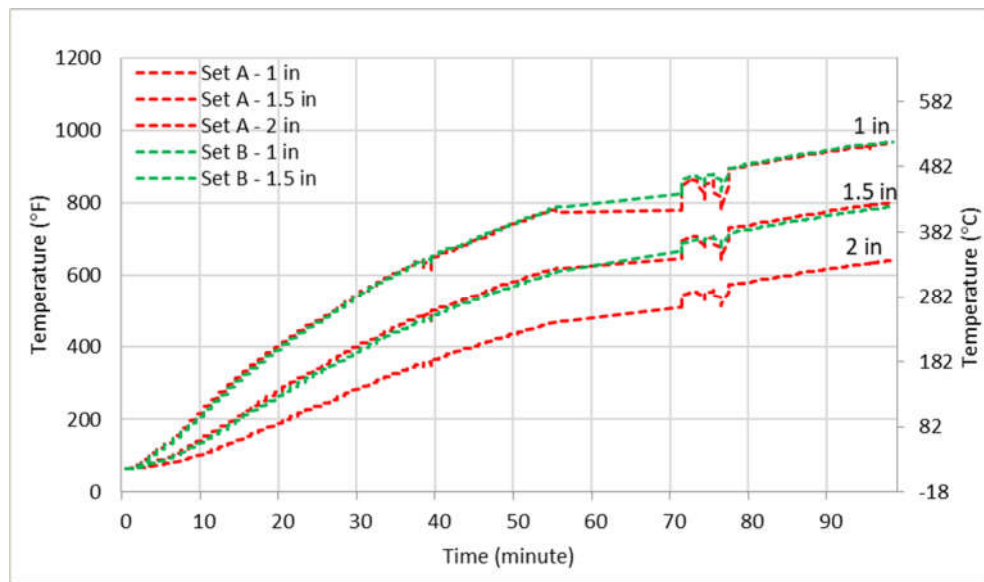

Figure 4-1. Temperature Profile Results

Figure 4-2 shows the surface temperature-time curves measured during the preliminary heating test, and compares them with: (i) the ISO-834 air temperature-time curve, and (ii) the

concrete surface temperature-time curves measured in standard furnace tests and reported in the literature. As shown in Figure 4-2, the surface temperature-time curves from the preliminary test were comparable to the concrete surface temperature-time curves from standard furnace tests reported in the literature by various researchers (Zheng 2008, Hou 2014, Rodrigues 2014. Thus, the high-temperature ceramic fiber radiant heaters used in the tests were able to simulate the heating associated with ISO-834 standard fire tests.
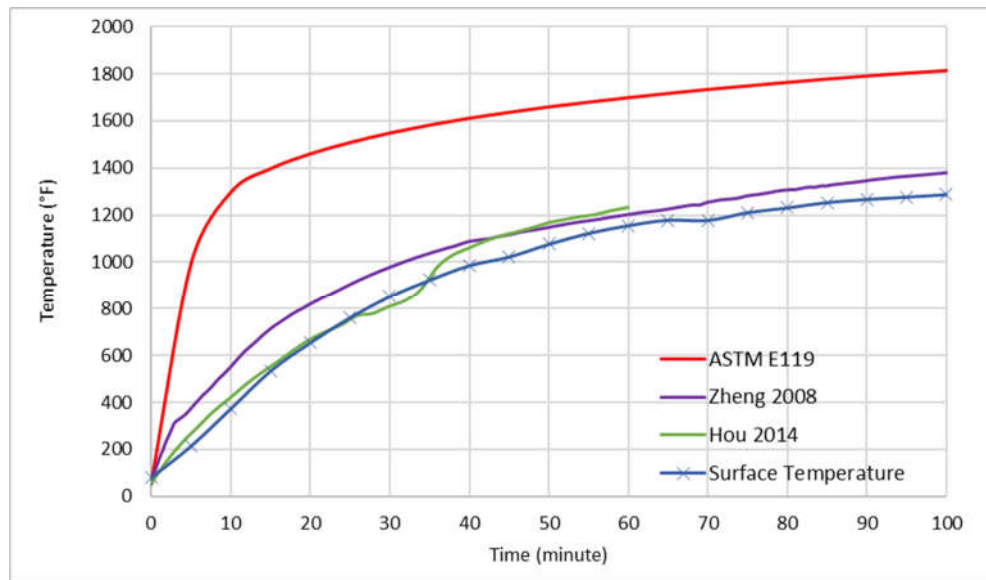

Figure 4-2. Surface Temperature Compared with Standard Fire Tests

Figure 4-3 compares the temperature-time histories from both sets of thermocouple trees with those reported by previous researchers. As shown, the temperature histories from the preliminary heating test compare reasonably with the temperature histories measured and reported within the concrete thickness by other researchers. This further verifies the heating approach and the temperatures measured by thermocouple trees installed before and after casting concrete.
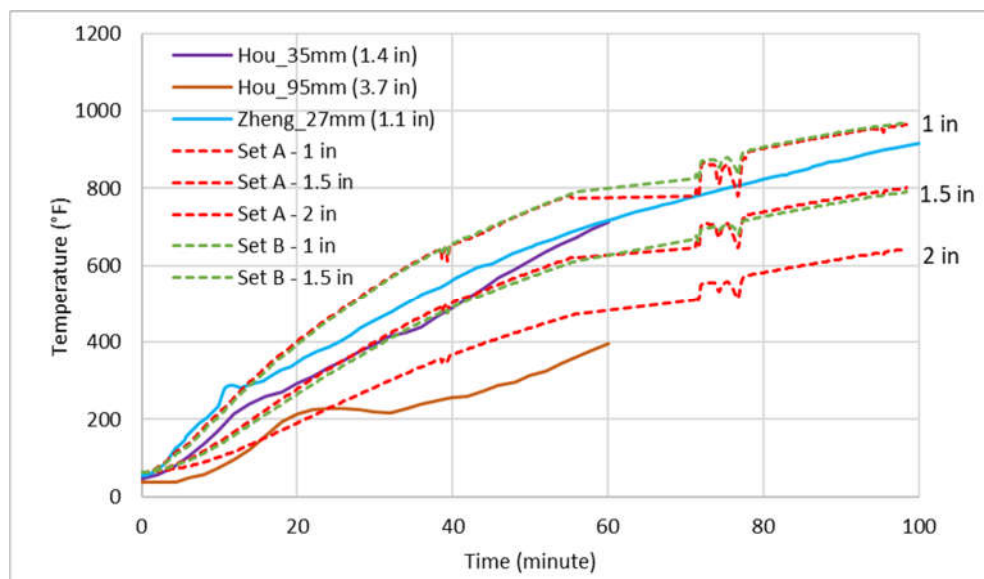
Figure 4-3. Through Depth Temperature Compared with Previous Research

Thus, the preliminary test verified the testing method, heating approach, and thermocouple installation process during and after concrete casting.

4.2.2 Deck Specimen Heating Test

This section discusses the observations and results from the testing of concrete deck specimens (48 in. by 48 in. by 8 in.) from the I-469 bridge over Feighner Road. The objectives of the series of tests are to evaluate the thermal and mechanical behavior of the specimen and to provide through-depth temperature profiles for concrete so that the microstructure degradation can be correlated with material analysis of the concrete samples taken from specimens. Each specimen is named as D – Test Duration in Minute – Maximum Surface Temperature in Fahrenheit. For example, D-40-1100 represents the deck specimen heated for 40 minutes to 1100°F (593°F) at the exposed surface. A summary table of names of deck specimens is shown in Table 4-1.

Table 4-1: Summary Table of Deck Specimen Names

Specimen Name	Duration of Heating
D-40-1100	40 Minutes
D-80-1600	80 Minutes

4.2.2.1   40-Minute Heating Test (D-40-1100)

The first experiment involved heating the deck specimen on one side for 40 minutes. The heaters were placed on the exposed surface of the deck specimen. During the experiment, moisture was observed at 16 minutes, when the surface temperature was around 600°F (316°C) and kept coming out till the end of the test. Figure 4-4 shows the observation of moisture from deck specimen during test. The locations with moisture were also observed to have cracks after the heating test.

At 16 Minutes– Surface Temperature: 600°F   At 36 Minutes – Surface Temperature: 1014 °F

Figure 4-4. Observation of Moisture from D-40-1100 during Test

After the test was finished, cracks on the exposed surface were observed and marked. It can be observed that cracks developed due to thermal expansion. As shown in Figure 4-5, thin cracks (< 0.005 in.) were observed. Most cracks were found along the locations of reinforcement bars, and some cracks extended into side face of the specimen. No spalling was found at the surface of concrete. Concrete color at some areas at exposed surface changed to darker grey after the heating test.

Figure 4-5. Map of Cracks for D-40-1100

The test ended at 40 minutes. After 40 minutes of heating, the maximum surface temperature of concrete reached to 1108°F (598°C), as shown in Figure 4-6.
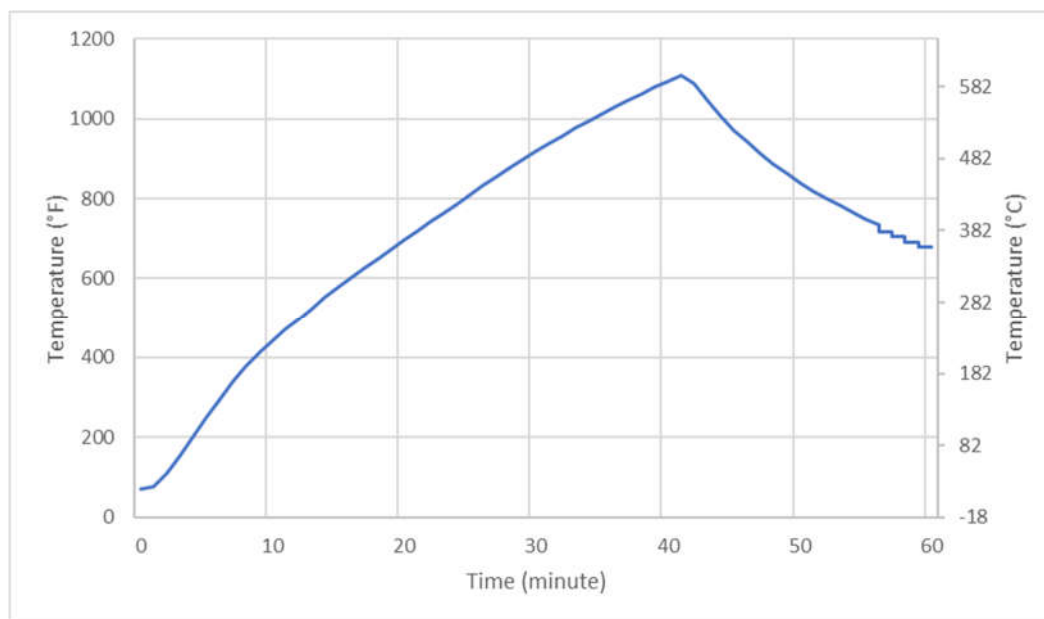

Figure 4-6. Surface Temperature Results of D-40-1100

The thermocouple tree was installed at the center of specimen. Temperature was measured through the depth from 0.25 in. to 2 in. Temperature profile of D-40-1100 is shown as Figure 4-7. Temperature at all depth increased constantly, with the same trend as surface temperature, till the end of test. Note that there is a plateau at around 200°F (93°C) due to the evaporation of free water from the concrete during heating.

At 40 minutes, maximum temperatures at 0.25 in., 0.5 in., 0.75 in., 1 in., 1.25 in., 1.5 in., and 2 in. are 903 °F, 786 °F, 673 °F, 557 °F, 493 °F, 395 °F, and 258 °F (484 °C, 419 °C, 356 °C, 292 °C, 256 °C, 202 °C, and 126 °C), respectively. As shown in Figure 4-7, none of the temperature results is great enough for limestone to decompose and quartz to change phase from α to β, which agrees with the observation on surface of specimen D-40-1100 that only thin cracks were found. Also, temperature results for up to 0.25 in. depth from exposed surface is greater than the temperature to decompose calcium hydroxide (CH), for which the loss of CH can cause debonding cracks and increase in porosity in the microstructure of concrete and reduction in strength.
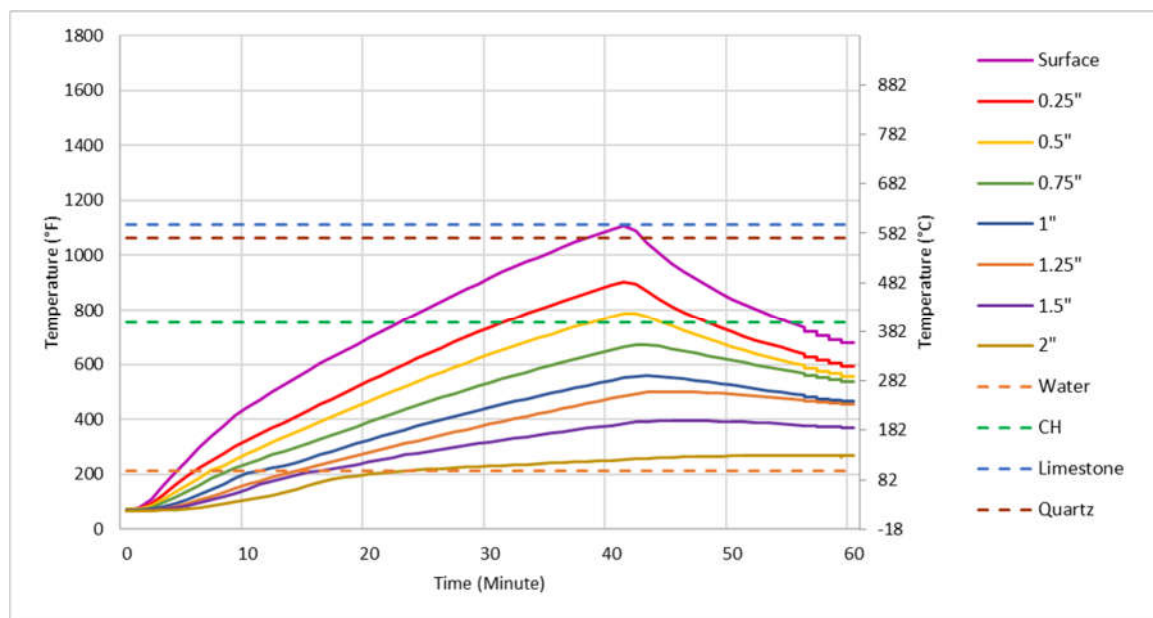

Figure 4-7. Through-Depth Temperature Results of D-40-1100

Vertical deflection results at center and quarter spans are shown in Figure 4-8. The location of each displacement transducer is shown in Figure 3-16. Deflection at the center (SS3) and quarter span (SS2) of D-40-1100 are 0.13 in. and 0.1 in respectively.
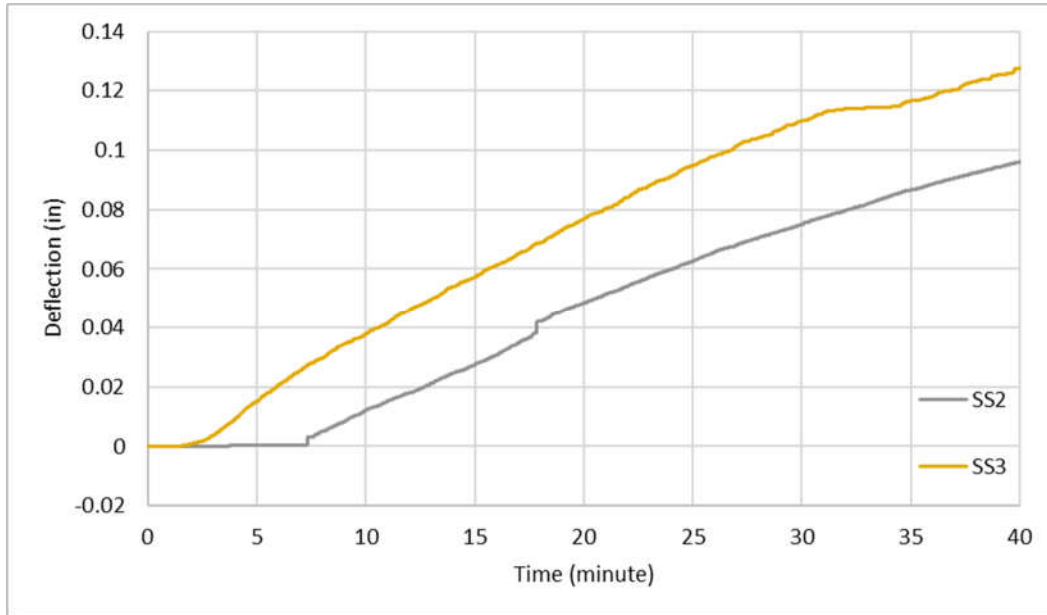

Figure 4-8. Results of Vertical Deflections of D-40-1100

4.2.2.2 80-Minute Heating Test (D-80-1600)

The third experiment involved heating the deck specimen on one-side for 80 minutes. During the experiment, moisture was observed at 15 minutes, when the surface temperature was around 600°F (316°C) and kept coming out till the end of the test. Figure 4-9 shows the observation of moisture from deck specimen during test. The locations with moisture were also observed to have cracks after the heating test.

At 15 Minutes– Surface Temperature: 626°F   At 76 Minutes – Surface Temperature: 1418°F

Figure 4-9. Observation of Moisture from D-80-1600 during Test

The locations of seeping moisture moved downward during heating. At the end of test, the average distance from the top of seeping points to the exposed surface was about 3 in, as shown in Figure 4-10.

Figure 4-10. Locations of Sweeping Moisture at One Side of D-80-1600

At 69 minutes, duct tape on one of the heaters caught fire due to extreme high temperature at the gap between heaters, as shown in Figure 4-11. All heaters were shut down for safety check and turned back on. The whole process lasted for one minute. This caused the decrease in temperature measurement, which can be also observed in Figure 4-13 and Figure 4-14.

Figure 4-11. Location of Fire during Test of D-80-1600

After the test was finished, cracks on the exposed surface was recorded. As shown in Figure 4-12, wide cracks (about 0.005 in.) were observed. Most cracks were found along the locations of reinforcement bars, and some cracks extended into side face of the specimen. Spalling was easily found at the exposed surface. After the spalling part was cleaned, more aggregates were exposed. Concrete color at some areas at exposed surface changed to yellowish grey color after the heating test.

Figure 4-12. Map of Cracks for D-80-1600

After 80 minutes of heating, the maximum surface temperature of concrete reached to 1631°F (888°C), as shown in Figure 4-13. The temperature increased smoothly during the 80-minute test, except that the temperature slightly dropped for about 100°F (38°C) due to the shutdown of heaters at 70 minutes. Based on the surface temperature result from Figure 4-13, it can explain that spalling was caused not only by the thermal expansion but also by the decomposition of carbonates. When the temperature reaches to above 1112°F (600 °C), limestone starts to decompose and forms lime and gas, which causes the spalling and reduction in strength.
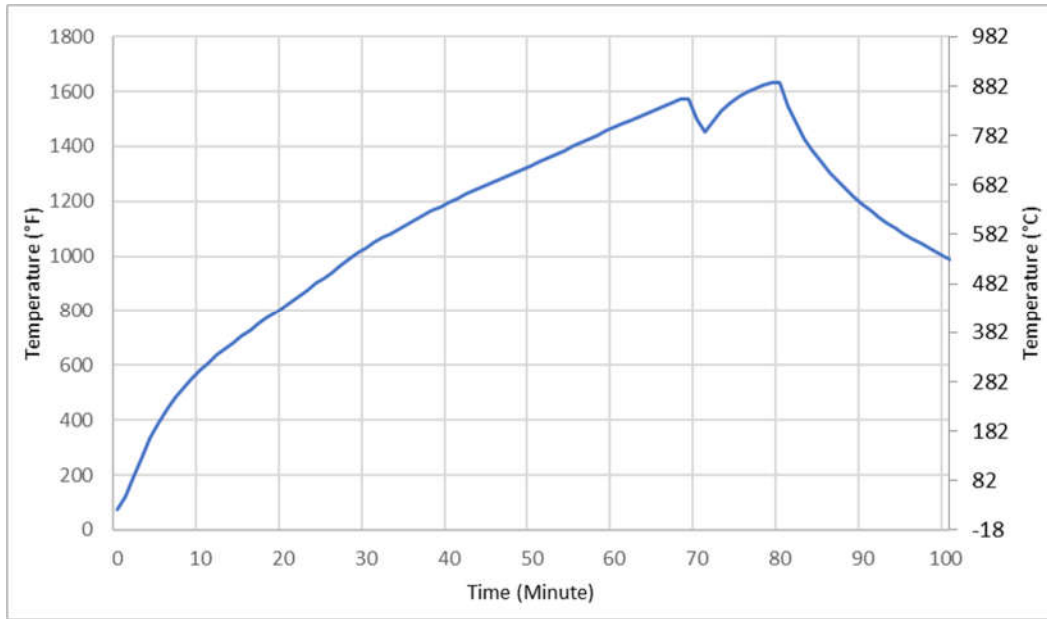
Figure 4-13. Surface Temperature Results of D-80-1600

The temperature from thermocouple tree was measured from 0.25 in. to 2 in. Through depth temperature profile of D-80-1600 is shown as Figure 4-14. Temperature at all depth increased constantly till the end of test. At 80 minutes, maximum temperatures at 0.25 in., 0.5 in., 0.75 in., 1 in., 1.25 in., 1.5 in., and 2 in. are 1169°F, 1080 °F, 973 °F, 880 °F, 772 °F, 691 °F, and 540 °F (632°C, 582°C, 523°C, 471°C, 411°C, 366°C, and 282°C), respectively. The shutdown of heaters at around 70 minutes caused the decrease in temperature till certain depth. As shown in Figure 4-14, temperature drop at 0.25 in. and 0.5 in. depth can be observed obviously. Comparing the temperature profile with the level of temperature of decomposition of particular particles, the temperature up to 0.25 in. from exposed surface is greater than the temperature for limestone to decompose and quartz to change phase from α to β. The phase change of quartz can cause volume change with additional cracking of the paste matrix. Also, temperature results for up to 1 in. depth from exposed surface is greater than the temperature to decompose calcium hydroxide (CH), for

which the loss of CH can cause debonding cracks in the microstructure of concrete and reduction
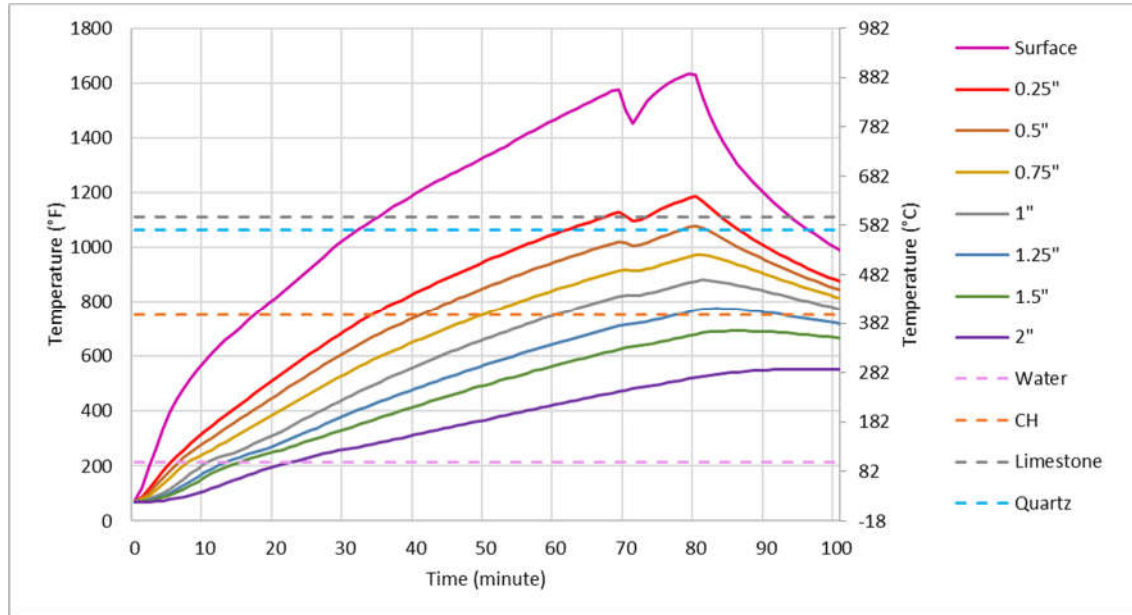
in strength.

Figure 4-14. Through-Depth Temperature Results of D-80-1600

Vertical deflection results at center and quarter spans for D-80-1600 are shown in Figure

4-15. The location of each slip sensor is shown in Figure 4-15. Deflection at the center (SS3) and

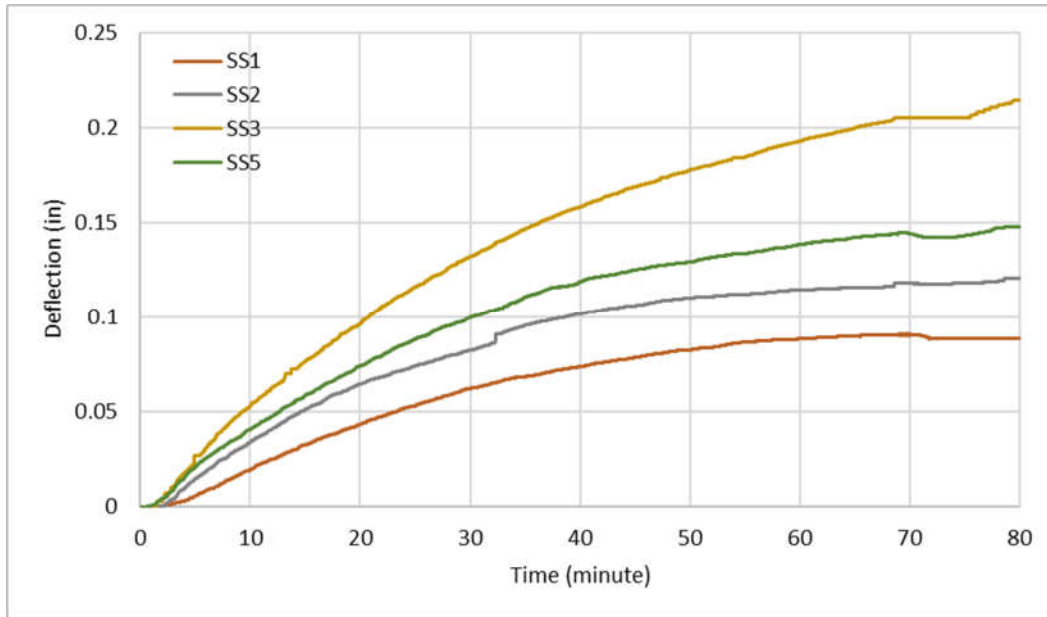quarter span (SS2) of D-80-1600 are 0.21 in. and 0.12 in respectively.

Figure 4-15. Results of Vertical Deflections of Deck Specimen

4.2.3 Comparison between 40-Minute and 80-Minute Heating Test Results

Figure 4-16 and Figure 4-17 show the comparisons of surface temperature and through thickness temperature between the 40-minute and 80-minute heating tests. As shown in Figure 4-16, the trend of surface temperature curve from 80 minutes of heating extends the trend of 40 minutes of heating.
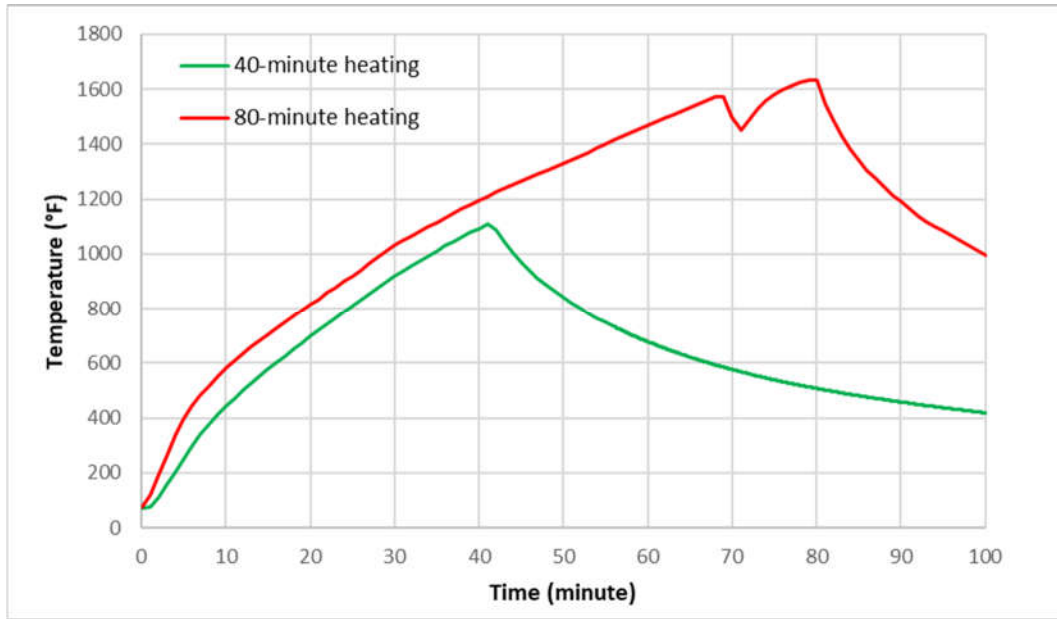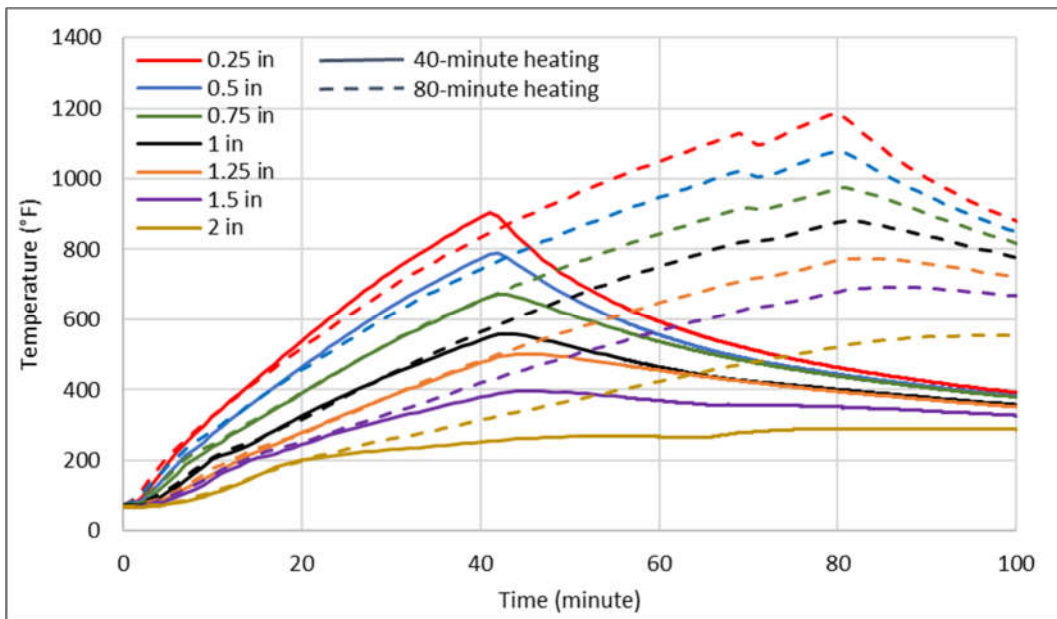
Figure 4-16. Comparison of Surface Temperature between 40 and 80 Minutes Tests

Figure 4-17. Comparison of Temperature Profiles between 40 and 80 Minutes Tests

Figure 4-18 and Figure 4-19 show the comparisons of vertical deflection results at center and quarter span between the 40-minute and 80-minute heating tests. As shown in Figure 4-18,

deflection at center of specimen increases with duration of heating. As shown in Figure 4-19, deflection at quarter span does not change much (less than 10%) with duration of heating.
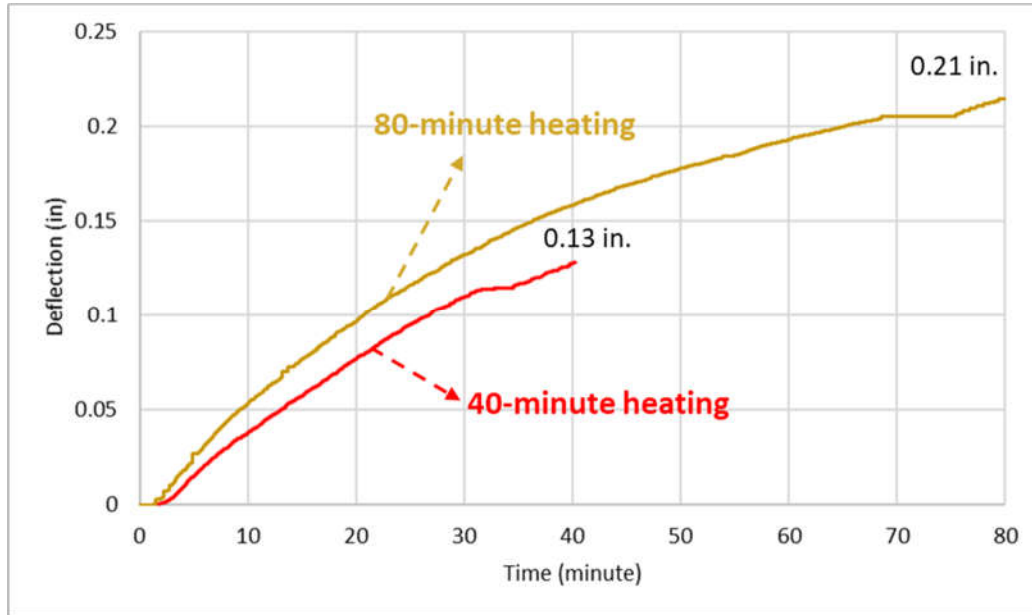

Figure 4-18. Comparison of Vertical Deflections at Center between 40 and 80 Minutes Tests
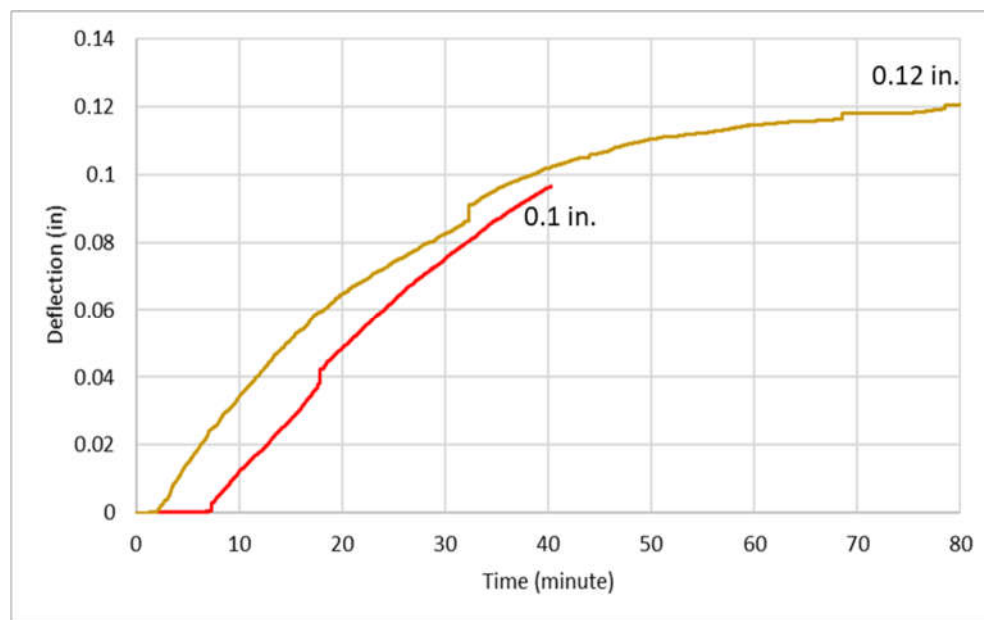

Figure 4-19. Comparison of Vertical Deflections at Quarter Span between 40 and 80 Minutes Tests

4.3   Material Experiment Results

Three methods of material analysis of concrete were used in this project to provide observations on the deck specimens from different perspectives. These three methods are Scanning Electron Microscopy (SEM), Energy Dispersive Spectroscopy (EDS), and Differential Scanning Calorimetry (DSC).

4.3.1 SEM/EDS Observations

Scanning Electron Microscope (SEM) is used to provide detailed information about the microstructure of concrete samples in terms of cracking, debonding of aggregates, and loss of phases by qualitative observations (i.e. calcium hydroxide, CH, in this case) of concrete specimens. Energy Dispersive Spectroscopy (EDS) is a method that can be applied during SEM analysis process to identify the presence and proportion of certain elements (e.g. calcium and oxygen elements inside CH) at certain points in the microstructure. This method is used to identify the presence of CH specifically in this project.

Prior to the heating experiment, one core was taken from the deck specimen for material analysis in order to compare with the cored samples to be taken after heating test. For simplification, samples were named as shown in Table 4-2. In order to correlate to the temperature profiles, important depths (i.e. exposed surface, 0.25 in., 0.5 in., 0.75 in., 1 in., 1.5 in., and 2 in.) were specifically observed during SEM and EDS analysis. For Unheated samples, since there is no fire happened, the observed depth was from exposed surface to 1 in. depth. For Heated – 40 and Heated – 80 samples, the observed depth was from exposed surface to 2 in. depth.
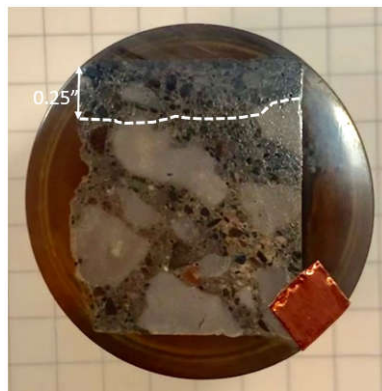
Table 4-2: Summary Table of SEM Sample Names

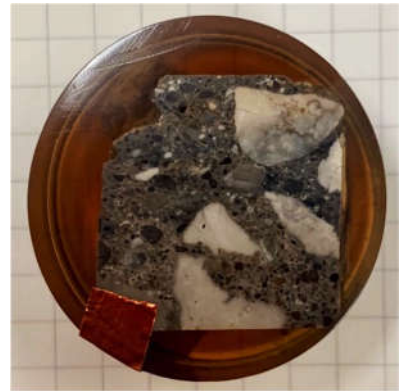| Sample Name	Duration of Heating
Unheated	Unheated
Heated – 40	40 Minutes
Heated – 80	80 Minutes

Figure 4-20 shows the visual observations of SEM samples. The color in Unheated sample is greyish color consistently through the depth. However, in Heated – 40 sample, at top part (around 0.25 in.) close to exposed surface, the color of concrete changes to darker grey, while the color in other locations looks similar as the Unheated sample. In Heated – 80 sample, the darker grey color extends to around 1 in. location. It can be inferred that the concrete whose color is changed is affected by the heating to the deck specimen at corresponding depth.
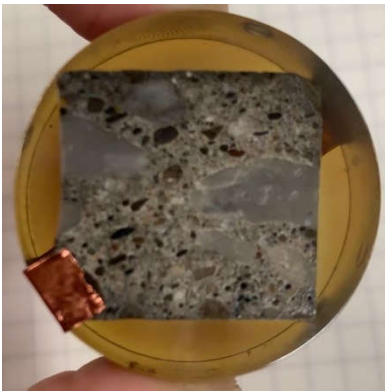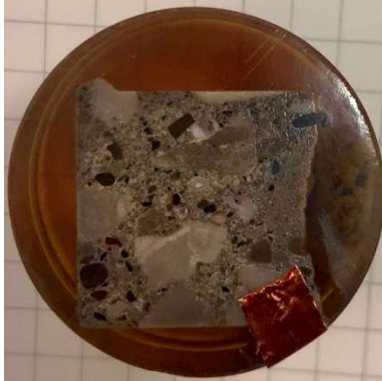

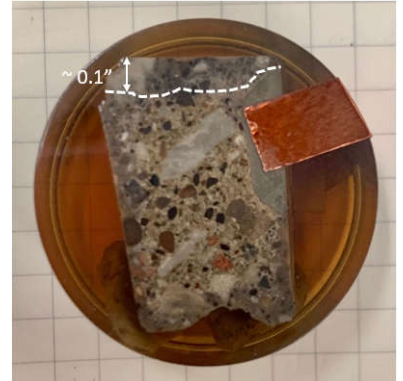(a). Unheated (Surface to 1 in.)   (b). Heated – 40 (Surface to 1 in.)   (c). Heated – 80 (Surface to 1 in.)
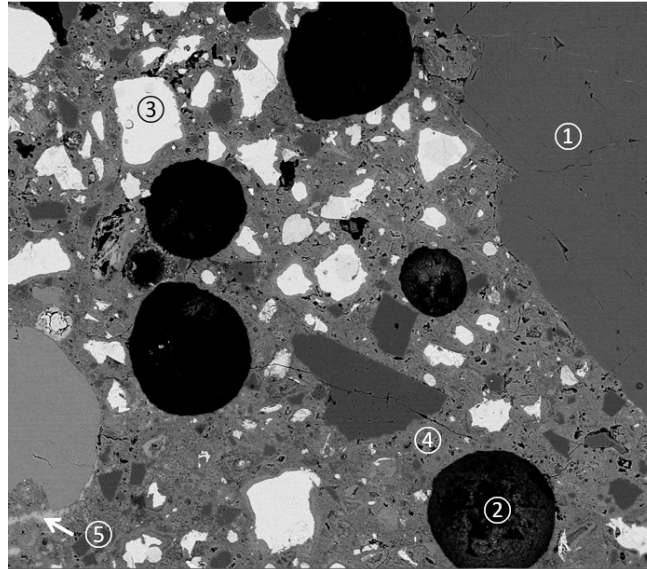
(d). Heated – 40 (1 in. to 2 in.)   (e). Heated – 80 (1 in. to 2 in.)

Figure 4-20. Visual Observations of SEM Samples

Figure 4-21 shows an example of SEM observation figures and explains the features of microstructure of concrete.

①: Aggregate ②: Pore ③: Unhydrated Cement ④: Paste Matrix ⑤: CH at Interfacial Transition Zone

Figure 4-21. Key for SEM Observations

Figure 4-22 shows an example of EDS identification. As shown in Figure 4-22, the spectrum shows that compositions at location 27 are mainly Ca and O, which indicates that the particle at location 27 is very possible CH ($Ca(OH)_2$). For simplification, EDS identifications in the following figures will only show the microstructure and locations of identified CH.
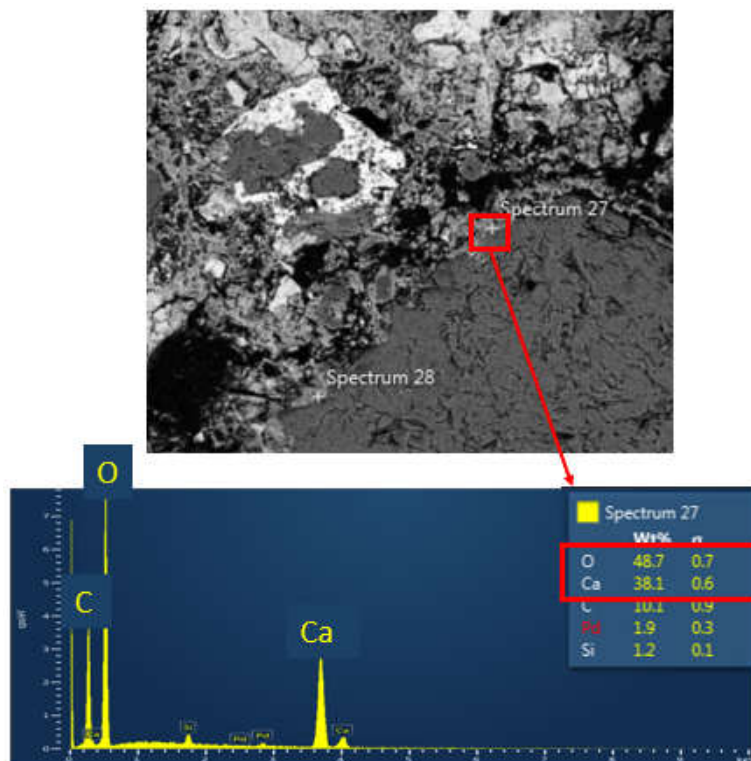
Figure 4-22. Example of EDS Identification

Figure 4-23 to Figure 4-29 show the SEM observations of microstructure of Unheated, Heated – 40, and Heated – 80 at various depths. In general, the paste in unheated sample is significantly more continuous and uniform than the paste in heated samples. For heated samples, the paste matrix observed at shallower location is more eroded and damaged compared with the one at deeper location. The porosity of paste matrixes increases with temperature at corresponding location increasing. More debonding cracks and pores can be found in the area with higher temperature. Thus, the elevated temperature evaporates the water from cement hydration particles, causes the absence of the bond between aggregates and paste, and increases the porosity of paste.

Observation of microstructure at exposed surface is shown in Figure 4-23. In Unheated sample, there are thin cracks along the paste and around the aggregate. Pores and unhydrated cement particles can be observed. The paste matrix is continuous. However, in Heated – 40 sample,
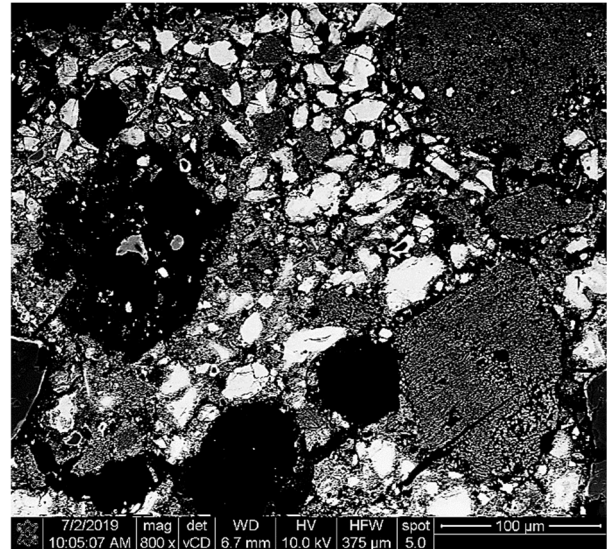
wide cracks and large pores can be found, and the paste looks eroded. In Heated – 80 sample, the paste almost disappears. Large debonding cracks and pores can be observed, and cracks connects pores together.
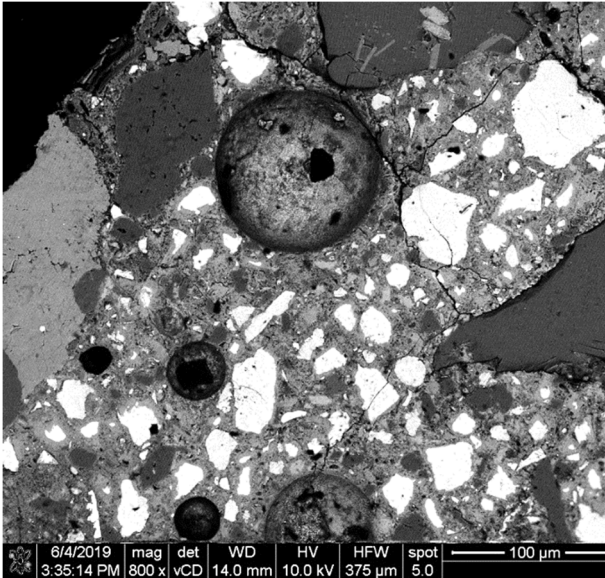
(a). Unheated
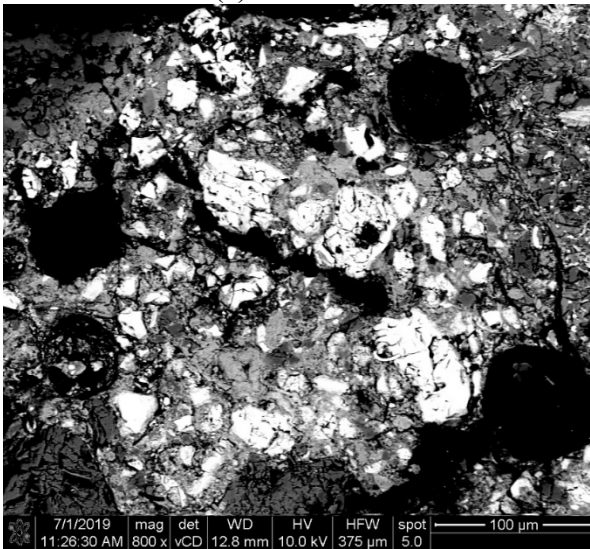
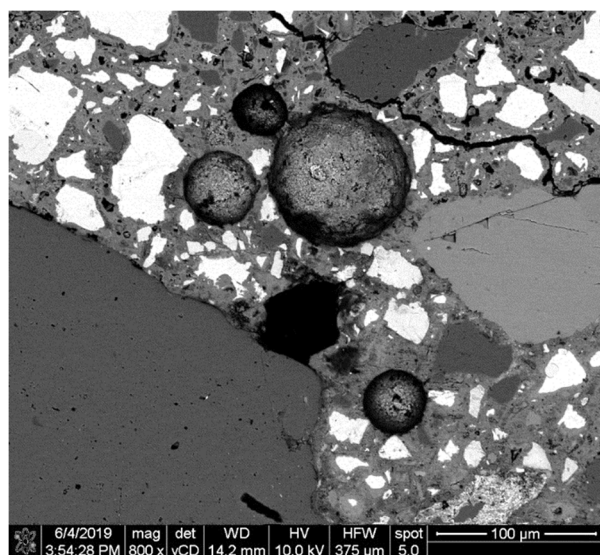(b). Heated – 40: 1108 °F (598 °C)
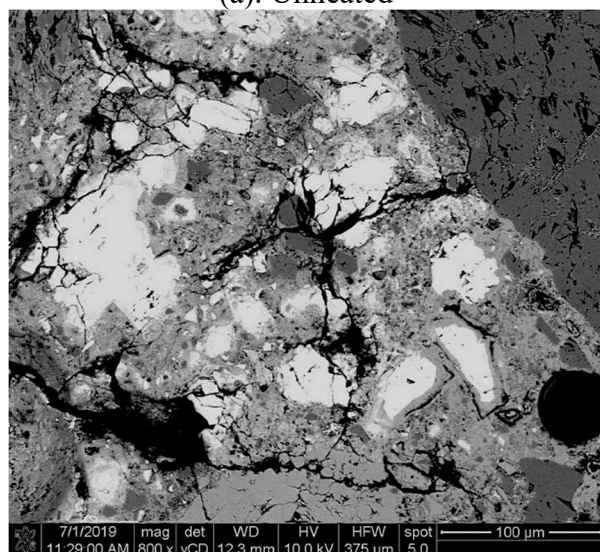

(c). Heated – 80: 1631 °F (888 °C)

Figure 4-23. SEM Observation of Microstructure of Concrete at Exposed Surface

Observation of microstructure at 0.25 in. is shown in Figure 4-24. In Unheated sample, a few cracks and pores are observed. The paste looks uniform. However, in Heated – 40 sample,
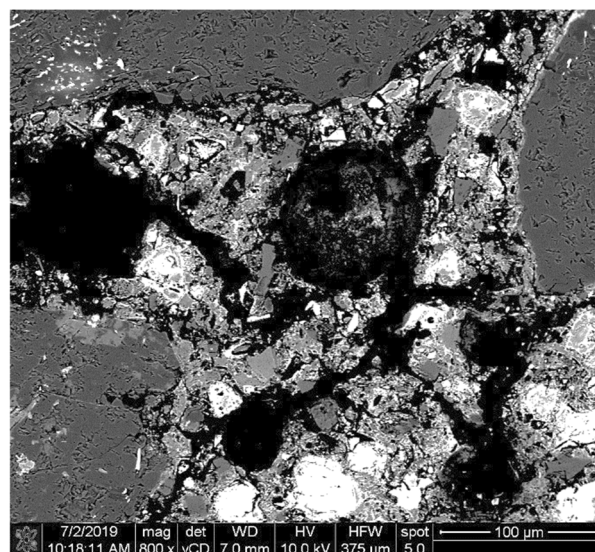
wide crack maps are observed throughout the paste, and debonding cracks can be easily found around aggregates. The paste looks porous. In Heated – 80 sample, crack maps become significantly wider, compared with Heated – 40. Large debonding cracks can be easily found. The paste looks very damaged.

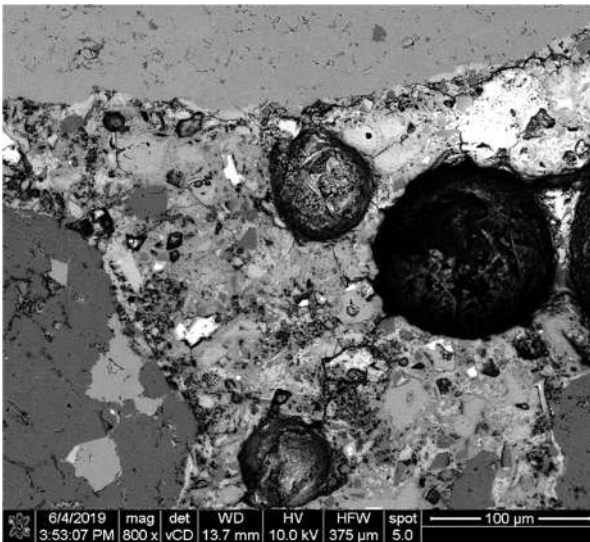(a). Unheated

(b). Heated – 40: 903 °F (484 °C)

(c). Heated – 80: 1169 °F (632 °C)

Figure 4-24. SEM Observation of Microstructure of Concrete at 0.25 in.

Observation of microstructure at 0.5 in. was shown in Figure 4-25. In Unheated sample, pores can be observed. Few fine cracks can also be found, but the paste matrix is generally

continuous. However, in Heated – 40 sample, a large horizontal crack is found in the figure. The paste is still porous, and many unhydrated cement particles are also observed, but less debonding cracks are found. In Heated – 80 sample, the paste is still eroded. It is evident to observe crack maps that are across the aggregate and pores, throughout the paste, and between aggregate and paste. Large pores can also be spotted.

(a). Unheated

(b). Heated – 40: 786 °F (419 °C)
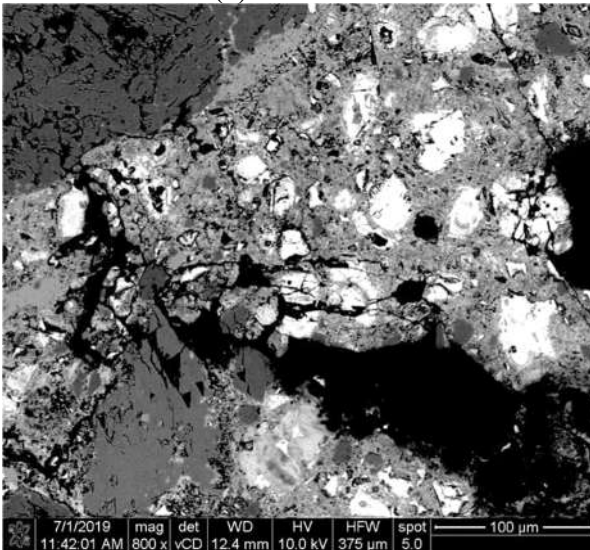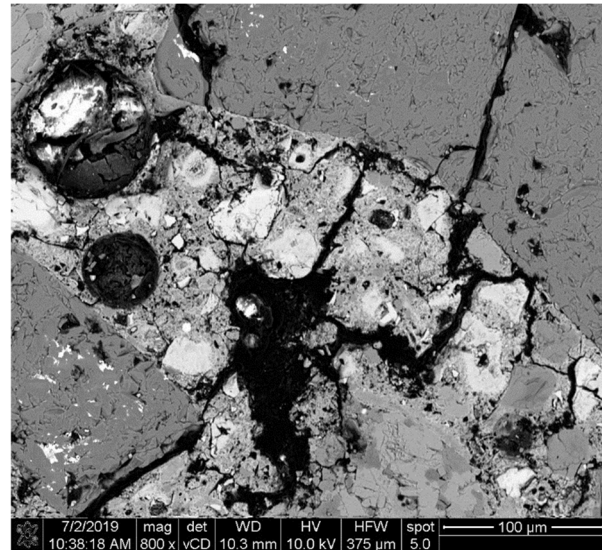

(c). Heated – 80: 1080 °F (582 °C)

Figure 4-25. SEM Observation of Microstructure of Concrete at 0.5 in.

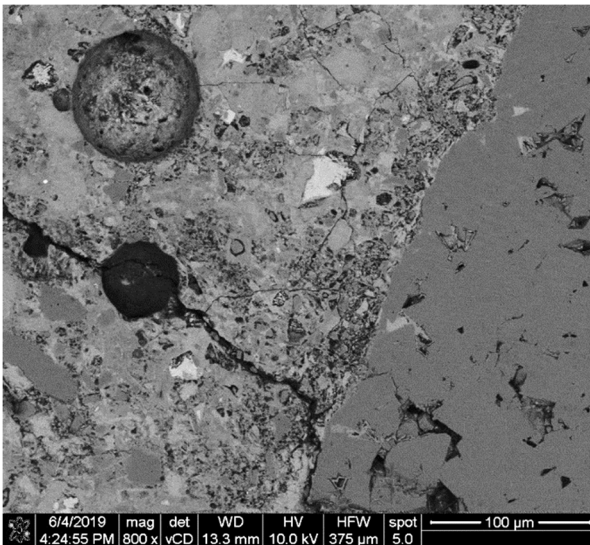Observation of microstructure at 0.75 in. was shown in Figure 4-26. In Unheated sample, a few cracks and pores are observed, but generally the paste matrix is uniform, and aggregates and paste are well bonded. In Heated – 40 sample, the microstructure looks smoother compared to the observations at shallower depth, but the paste is still more porous than that in Unheated sample. A few cracks and pores can be found. In Heated – 80 sample, the paste is very porous. Large debonding cracks and pores can be easily observed.
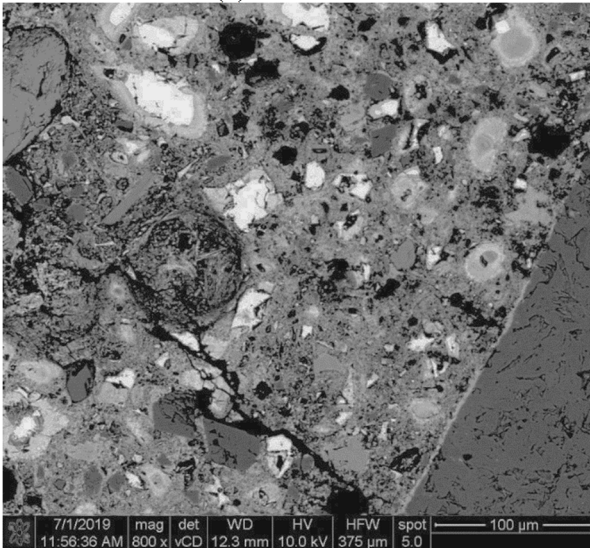

(a). Unheated

(b). Heated – 40: 673 °F (356 °C)

(c). Heated – 80: 973 °F (523 °C)

Figure 4-26. SEM Observation of Microstructure of Concrete at 0.75 in.

Observation of microstructure at 1 in. was shown in Figure 4-26. In Unheated sample, the paste is smooth and uniform. Few cracks and pores can be found. Aggregates and paste are well bonded. In Heated – 40 sample, the paste is less porous compared with the paste above. A few cracks can be spotted, but in general the microstructure seems unaffected. In Heated – 80 sample, the paste is less porous than above. However, large debonding cracks and crack maps can still be observed throughout the paste.

(a). Unheated

(b). Heated – 40: 557 °F (292 °C)

(c). Heated – 80: 880 °F (471 °C)

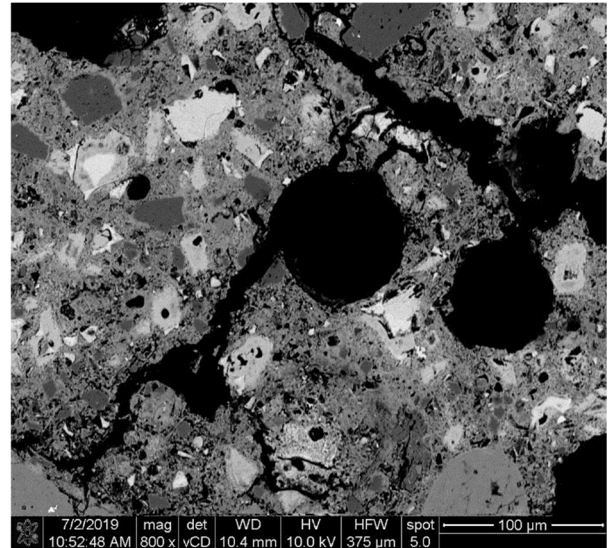Figure 4-27. SEM Observation of Microstructure of Concrete at 1 in.

Observation of microstructure at 1.5 in. was shown in Figure 4-28. In Heated – 40 sample, the paste is very consistent. A few cracks and pores can be spotted, but in general the microstructure is unaffected by heating. In Heated – 80 sample, the paste is continuous as well. Even though there are still small debonding cracks and pores, the microstructure looks similar as the Unheated sample.
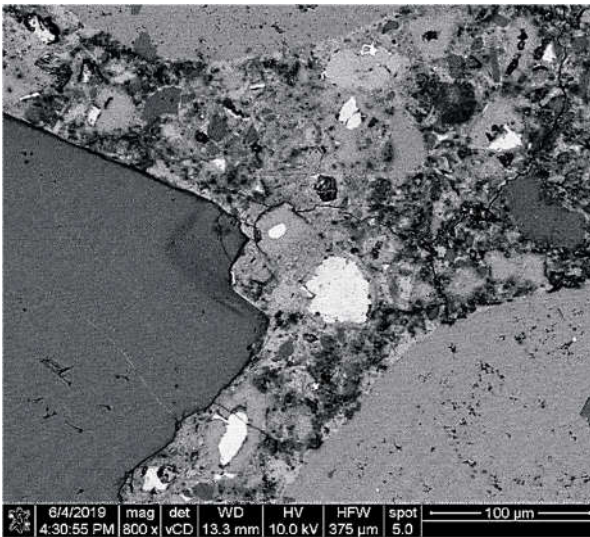

(b). Heated – 40: 395 °F (202 °C)   (c). Heated – 80: 691 °F (366 °C)
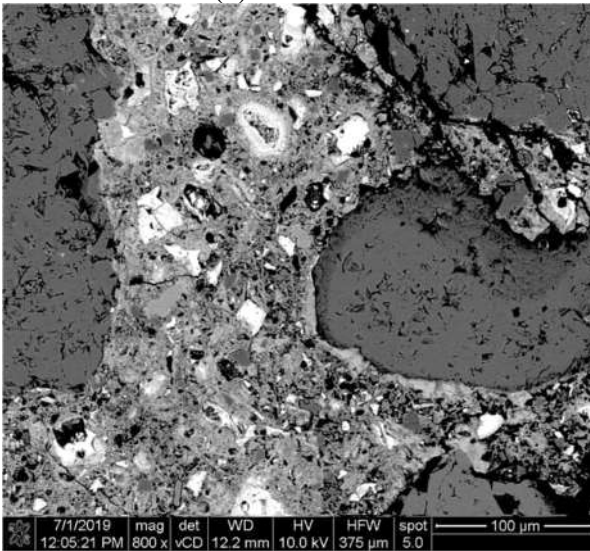
Figure 4-28. SEM Observation of Microstructure of Concrete at 1.5 in.

Observation of microstructure at 2 in. was shown in Figure 4-26. Heated – 40 and Heated – 80 samples are very comparable. For both samples, the paste is very uniform. A few pores and cracks can be spotted, but the microstructures are unaffected and similar as the Unheated sample.

(b). Heated – 40: 258 °F (126 °C)   (c). Heated – 80: 540 °F (282 °C)

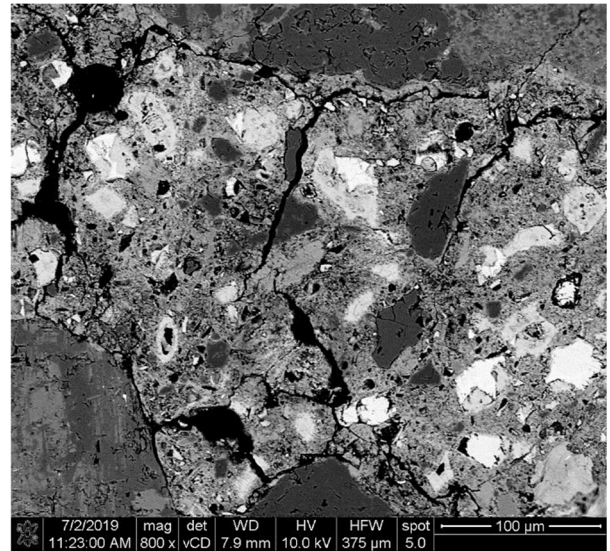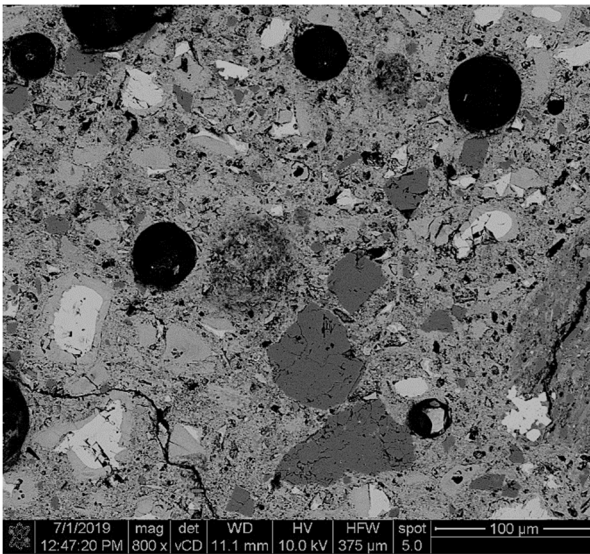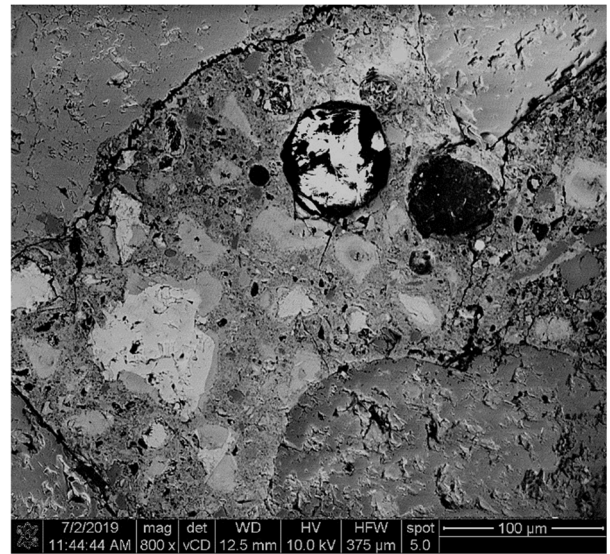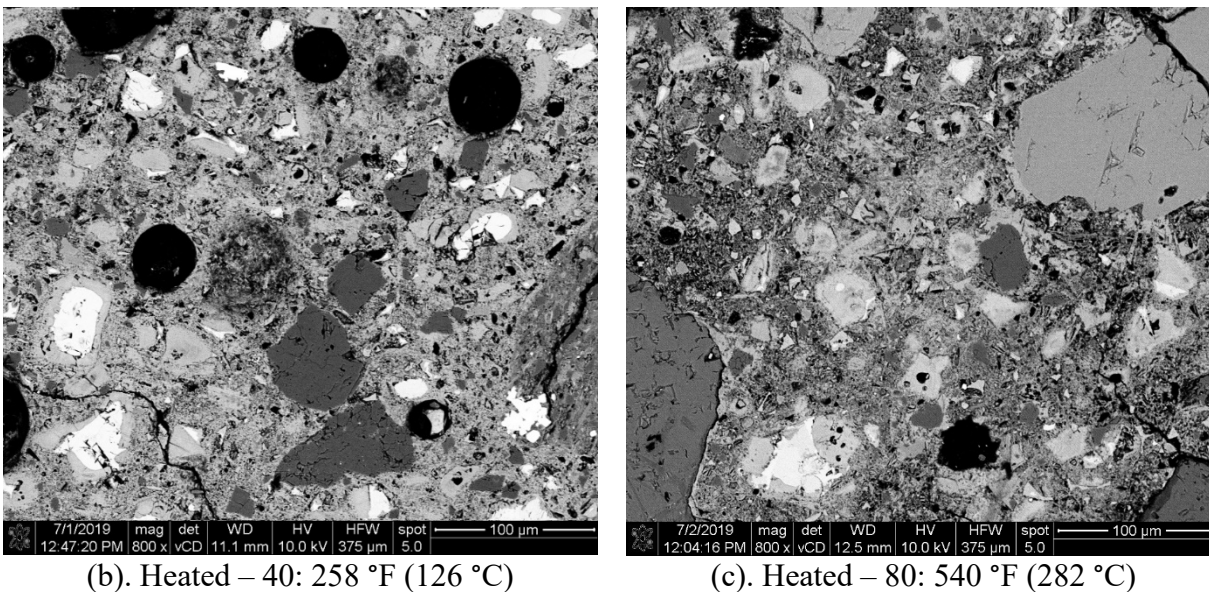Figure 4-29. SEM Observation of Microstructure of Concrete at 2 in.

Figure 4-30 to Figure 4-36 show the EDS identification of calcium hydroxide (CH) in the microstructure of Unheated, Heated – 40, and Heated – 80 at various depths. Normally, CH exists in interfacial transition zones (ITZs) between the aggregates and the paste in the concrete, which is shown as bright greyish color in the EDS figures. The presence of thin film of CH provides bonds between the aggregates and the pastes so that concrete can remain its strength. With temperature rising and moisture evaporating, CH loses water and disappears, which is also an indicator of temperature at certain depth of concrete. CH will be hard to find if temperature reaches to 752°F to 932°F (400°C to 500°C) and lasts for more than 20 minutes.

As one can tell from Figure 4-30 to Figure 4-36, the presence of CH is much easier to observe in unheated sample than in heated samples. It is also easier to find CH at deeper location through the depth of concrete than at shallower location. At exposed surface, even for Unheated sample, CH is hard to observe and mainly carbonated due to long time exposure to weather during the service life of the bridge deck.

Figure 4-30 shows the EDS identification of CH at exposed surface in Unheated sample. CH is carbonated and can only be found around pores. CH at exposed surface of Unheated sample is very limited. No sign of CH can be observed at exposed surface of Heated – 40 or Heated – 80 samples due to exposure to heat for long time duration.

Figure 4-30. EDS Identification of CH of Unheated Sample at Exposed Surface

Figure 4-31 shows EDS identification of CH at 0.25 in. In Unheated sample, CH can be found in ITZs but is mainly carbonated. In Heated – 40 sample, CH can only be found in few ITZs. Also, the large debonding cracks around aggregates indicate the loss of CH due to heating. In Heated – 80 sample, CH is barely left in ITZs. Large cracks and pores are around aggregate, which also implies the absence of CH.
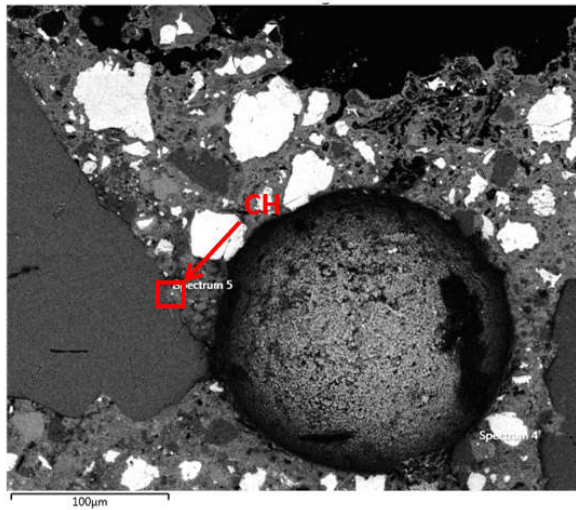
(a). Unheated
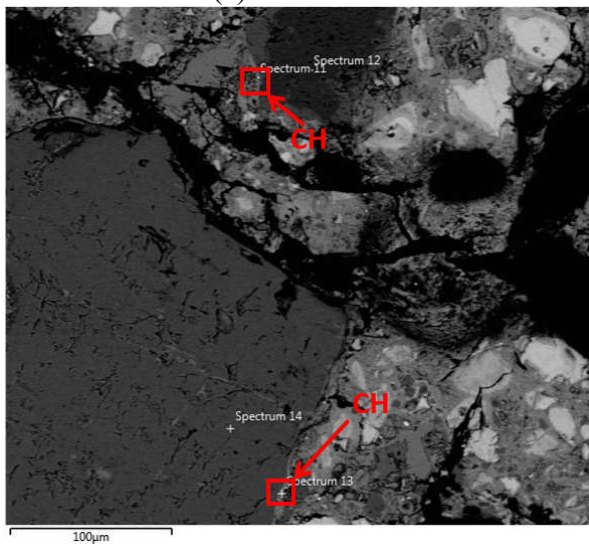
(b). Heated – 40: 903 °F (484 °C)
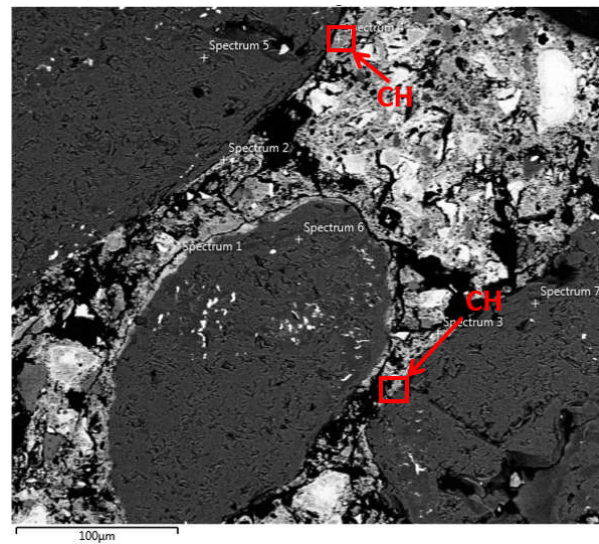
(c). Heated – 80: 1169 °F (632 °C)

Figure 4-31. EDS Identification of CH at 0.25 in.

Figure 4-32 shows EDS identification of CH at 0.5 in. In Unheated sample, CH can be easily found in ITZs and around pores. Also, around aggregates, large field of CH can be observed. In Heated – 40 sample, CH can hardly be found around pores or in ITZs. In Heated – 80 sample, minimal CH can be observed around pores. Large cracks across and around aggregates also implies lack of moisture and loss of CH at 0.5 in depth.

(a). Unheated

(b). Heated – 40: 786 °F (419 °C)
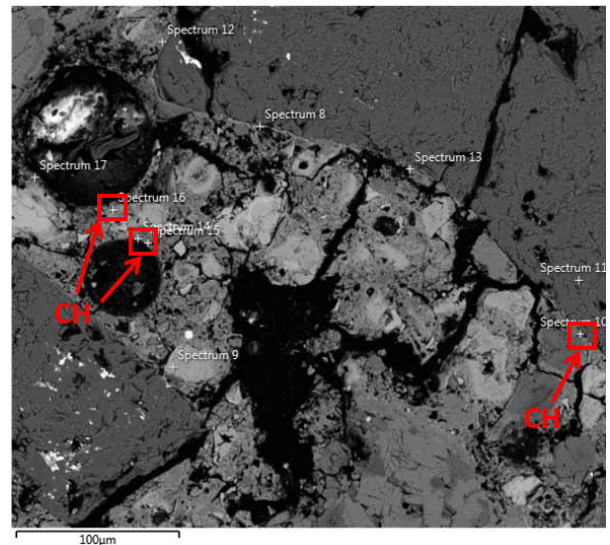
(c). Heated – 80: 1080 °F (582 °C)

Figure 4-32. EDS Identification of CH at 0.5 in.

Figure 4-33 shows EDS identification of CH at 0.75 in. In Unheated sample, large field of CH can be easily found in ITZs, shown as white dashed lines in the figure. In Heated – 40 sample, CH becomes more observable than above. Adequate CH are spotted in ITZs and around pores. In Heated – 80 sample, the paste is still very porous, and minimal CH can be observed around pores.

(a). Unheated
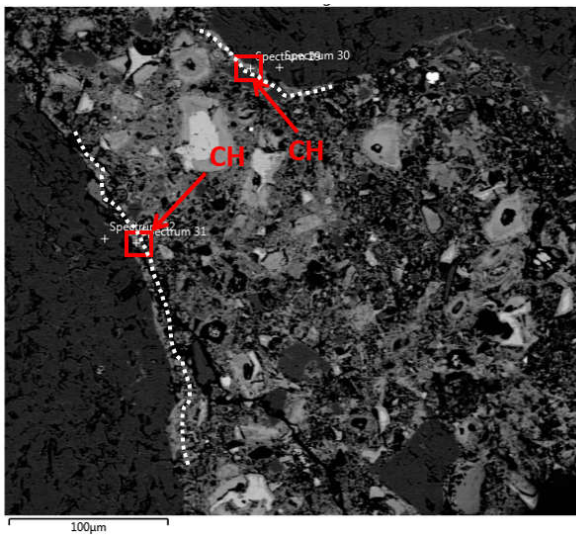
(b). Heated – 40: 673 °F (356 °C)
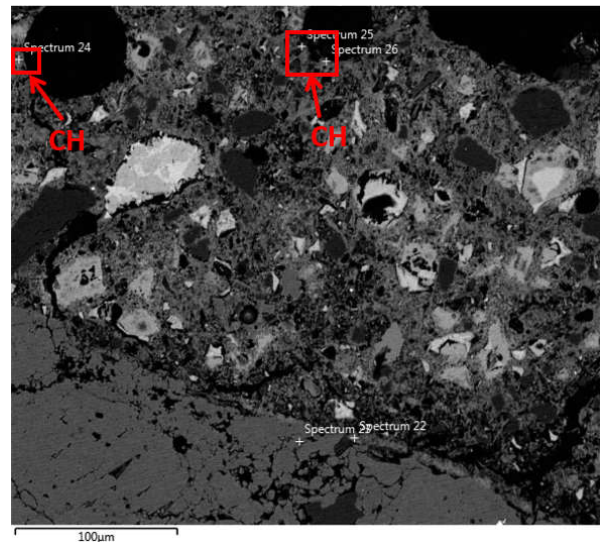
(c). Heated – 80: 973 °F (523 °C)

Figure 4-33. EDS Identification of CH at 0.75 in.

Figure 4-27 shows EDS identification of CH at 1 in. In Unheated sample, CH is sufficient and can be found in ITZs and around pores. In Heated – 40 sample, the presence of CH is observed in ITZs. In Heated – 80 sample, large cracks still exist around aggregates. Few CH is observed along the cracks, and the damaged microstructure indicates that the moisture is evaporated at 1 in. and CH is absent in most ITZs.
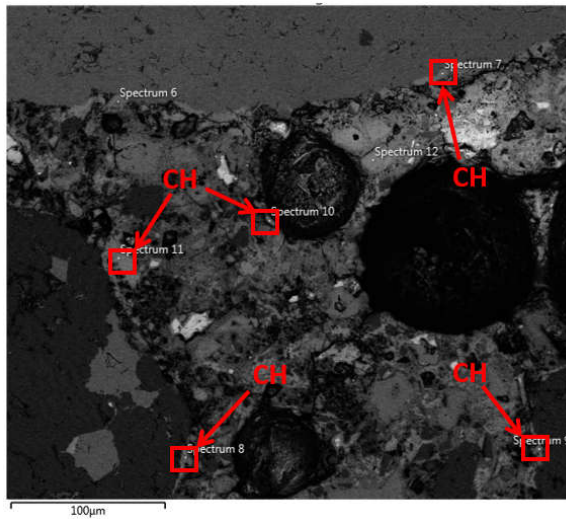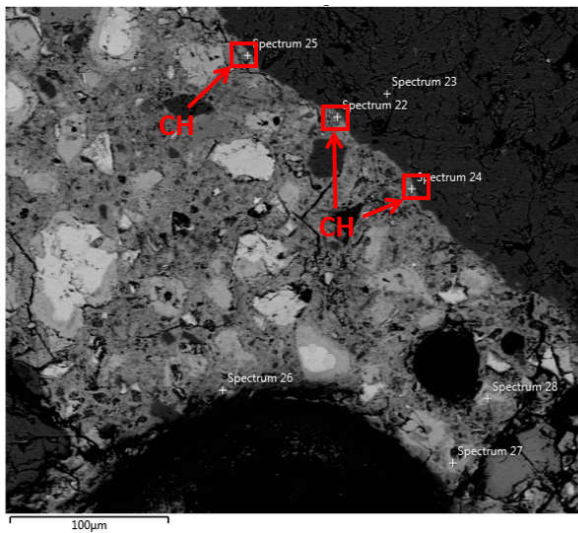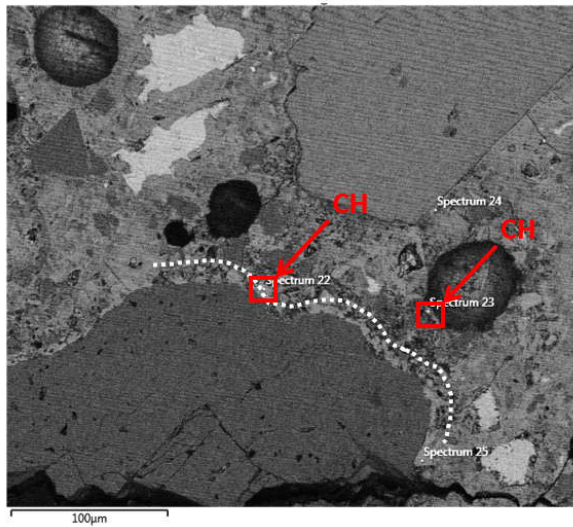
(a). Unheated
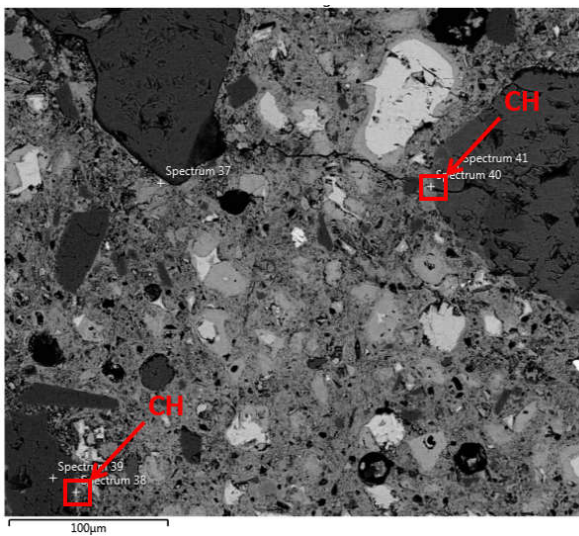
(b). Heated – 40: 557 °F (292 °C)
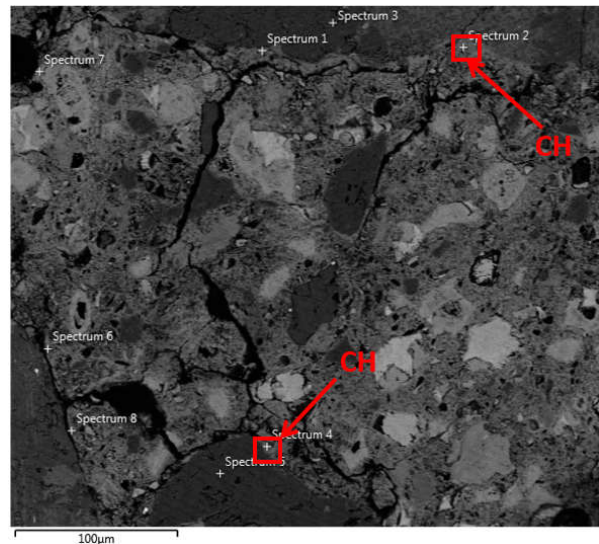
(c). Heated – 80: 880 °F (471 °C)

Figure 4-34. EDS Identification of CH at 1 in.

Figure 4-35 shows EDS identification of CH at 1.5 in. In Heated – 40 sample, CH is easy to observe. CH is present in ITZs and around pores. In Heated – 80 sample, more CH can be found at 1.5 in. CH is located around pores and aggregates. At this depth, the microstructure is not much affected by the heating.
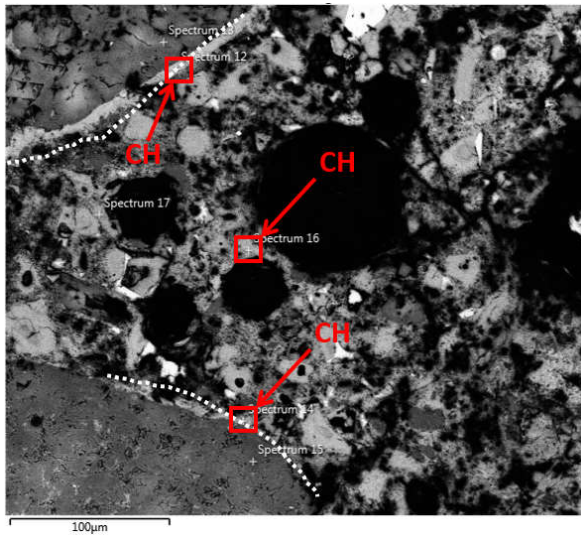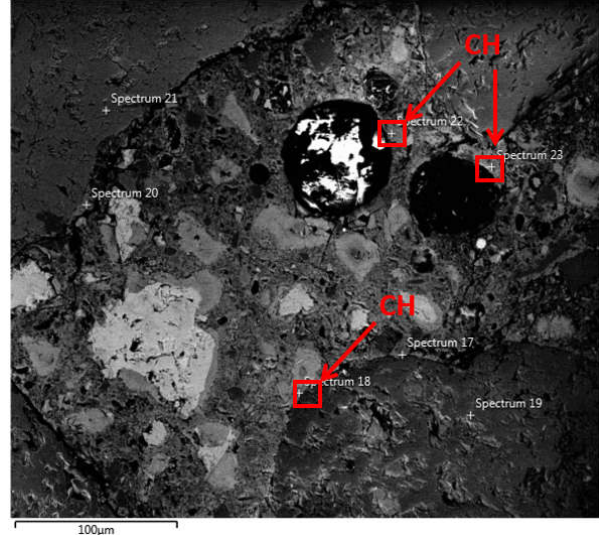
(b). Heated – 40: 395 °F (202 °C)   (c). Heated – 80: 691 °F (366 °C)
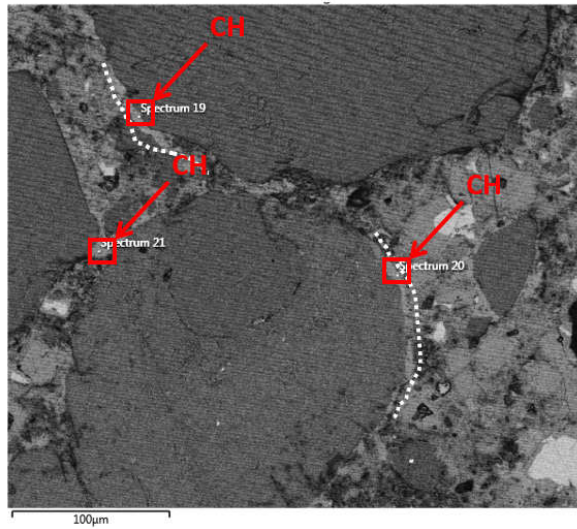
Figure 4-35. EDS Identification of CH at 1.5 in.

Figure 4-36 shows EDS identification of CH at 2 in. In both Heated – 40 and Heated – 80 sample, CH is easily observable, in ITZs and around pores, which indicates that the microstructure is unaffected by heating at 2 in.
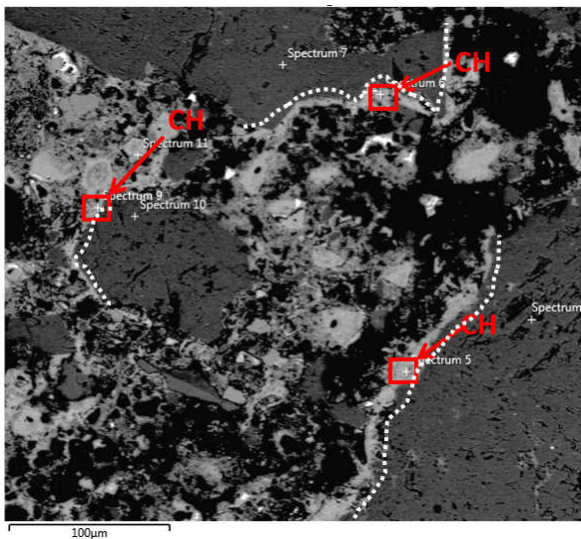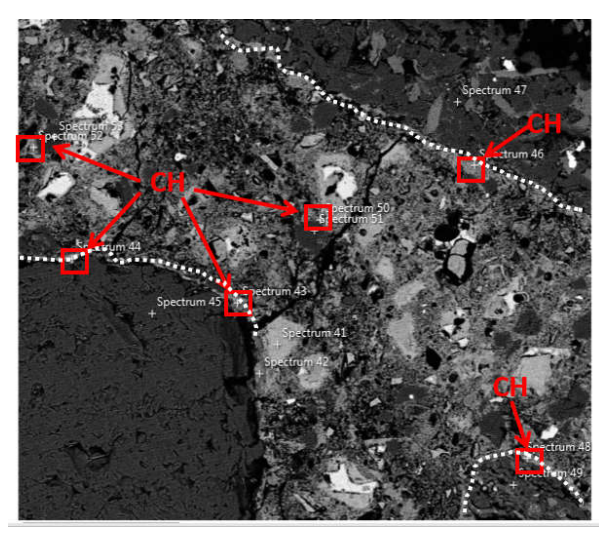
(b). Heated – 40: 258 °F (126 °C)   (c). Heated – 80: 540 °F (282 °C)

Figure 4-36. EDS Identification of CH at 2 in.

4.3.2 DSC Analysis

Differential Scanning Calorimetry (DSC) is a material analysis method to quantify the content of various phases (i.e. CH in this case) and to indicate the impact of fire on characteristics of cement paste. The content of certain phases is calculated based on the area of the peak associated with heat flow required to decompose this particular phase. Thus, DSC can provide quantitative estimation of the percent of CH remained at certain level of the deck specimen.

In order to quantify the content of CH and provide a reference for DSC analysis on the collected samples from deck specimens, a calibration curve of the content of CH is produced by mixing fired kaolinite (with no CH content inside) with calcium hydroxide powder with various ratios and measuring the heat flow of 0% CH (100% fired kaolinite), 10% CH, 20% CH, 50% CH, and 100% CH, as shown in Figure 4-37.
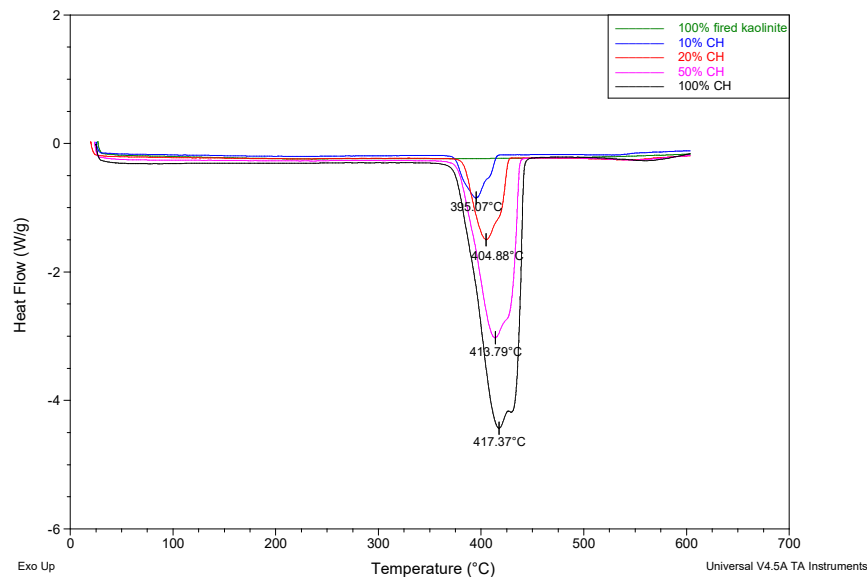
Figure 4-37. Calibration Curve of the Content of CH

From Figure 4-37, the peak area can then be calculated at each percent of CH. The percent of CH is plotted with the peak area, as shown in Figure 4-38. A trendline (with R^2 = 0.99) is generated from Figure 4-38 to provide an estimation of CH content in the samples.
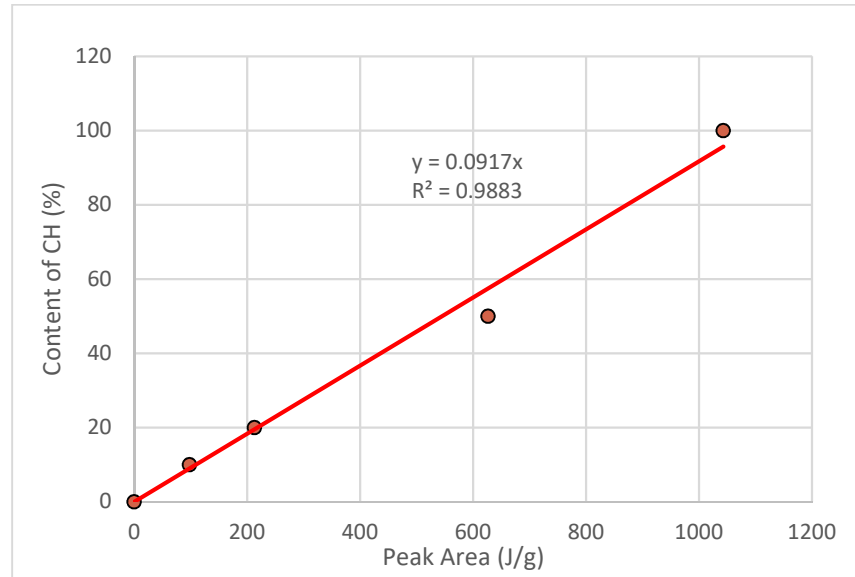
Figure 4-38. Calibration Equation of Content of CH

Thus, content of CH can be calculated using the equation below:

Content of CH (%) = 0.0917 x Peak Area (J/g)

Both unheated and heated samples were tested in DSC analysis in order to indicate the effect of fire on the paste of concrete from deck specimens. Same as SEM analysis, samples were named as Unheated, Heated – 40, and Heated – 80 to represent for unheated samples, samples heated to 40 minutes, and samples heated to 80 minutes. In order to match with the temperature profiles, important depths (i.e. 0.25 in., 0.5 in., 0.75 in., 1 in., 1.5 in., and 2 in.) were specifically tested during DSC analysis. Note that DSC results at 0.25 in. means the sample was the average within the range from exposed surface to 0.25 in. depth, 0.5 in. means the sample was the average

within the range from 0.25 in. to 0.5 in. depth, etc. The maximum temperature values at corresponding depths during heating experiments is shown in Figure 4-39.
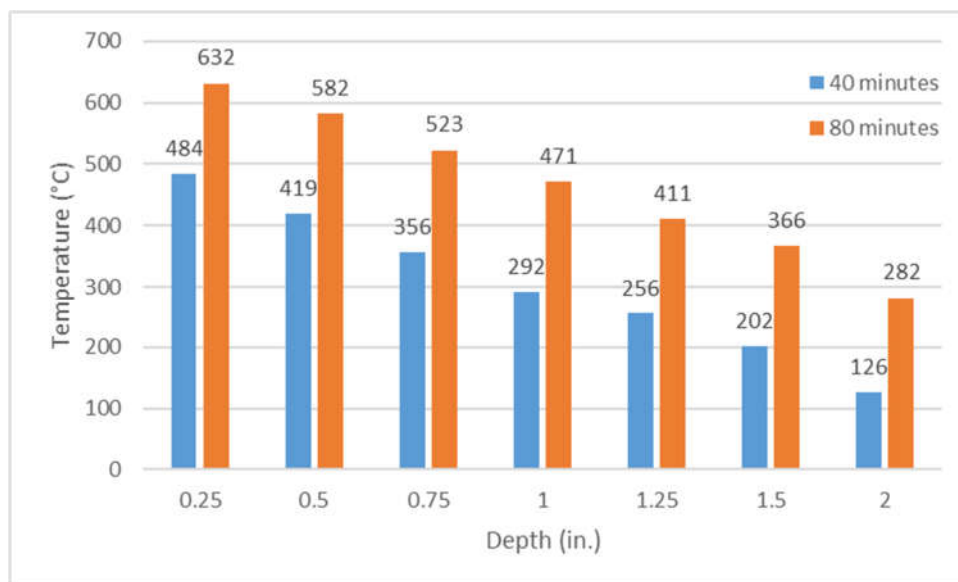
Figure 4-39. Temperature Values at Certain Depth at the End of Heating Tests

Figure 4-40 to Figure 4-42 show the change of heat flow in concrete with regard to temperature change, from unheated and heated samples. Two main peak zones can be found: one is at around 212°F (100°C) and the other one is at 754°F to 932°F (400 °C to 500 °C). The initial peak at around 100 °C indicates the change of energy associated with water evaporation, which indicates the temperature at certain depth but does not cause the reduction in strength. The peak at 400 °C to 500 °C reflects the decomposition of hydrates (i.e. CH in this case), when most of cements become dehydrated. This peak is important for the study and will be discussed in detail in this subsection.

Figure 4-40 shows the DSC analysis results for Unheated sample. As shown in Figure 4-40, the peak of 0.25 in. curve around 400 °C to 500 °C is smaller than curves from depths beyond. This illustrates that less CH can be found at exposed surface even before heating, because of the

carbonation at the surface. Beyond 0.5 in., the peaks are similar, which explains the effect of carbonation becomes not as significant. This result also agrees with the SEM observations of Unheated sample.
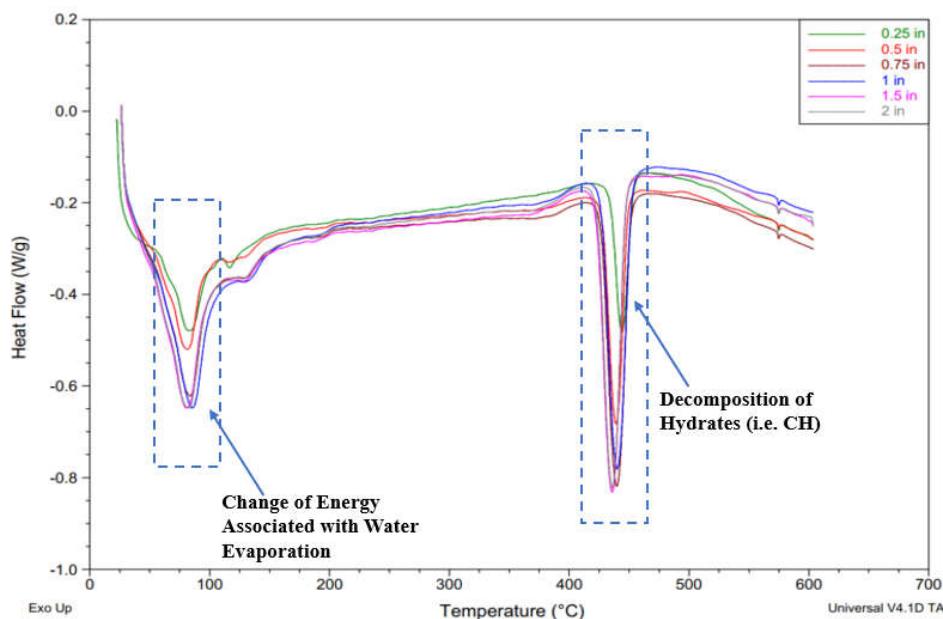
Figure 4-40. DSC Analysis Results of Unheated Sample

Figure 4-41 shows the DSC analysis results of Heated – 40 sample at various depths. One can tell that the peak for 0.25 in. is significantly smaller than curves from depth beyond and corresponding curve in Unheated sample, which means that there is barely any CH decomposed at 0.25 in. during DSC analysis. As a result, CH at 0.25 in. depth was totally decomposed during the 40 minutes heating test. Beyond 0.25 in. depth, rest of the curves were very comparable with Unheated sample. Thus, from DSC analysis, it is estimated that, for 40 minutes heating, the heat has affected the composition of CH and the strength of concrete till 0.25 in. Also, the maximum heat flows for peaks at 100 °C of Heated – 40 are much smaller than the peaks of Unheated sample analysis results, which illustrates the dehydration of Heated – 40 sample up to 2 in. Even though

the temperature for 40 minutes heating is not high enough to decompose CH, the temperature up to 2 in. is still adequate to evaporate water during the heating test.
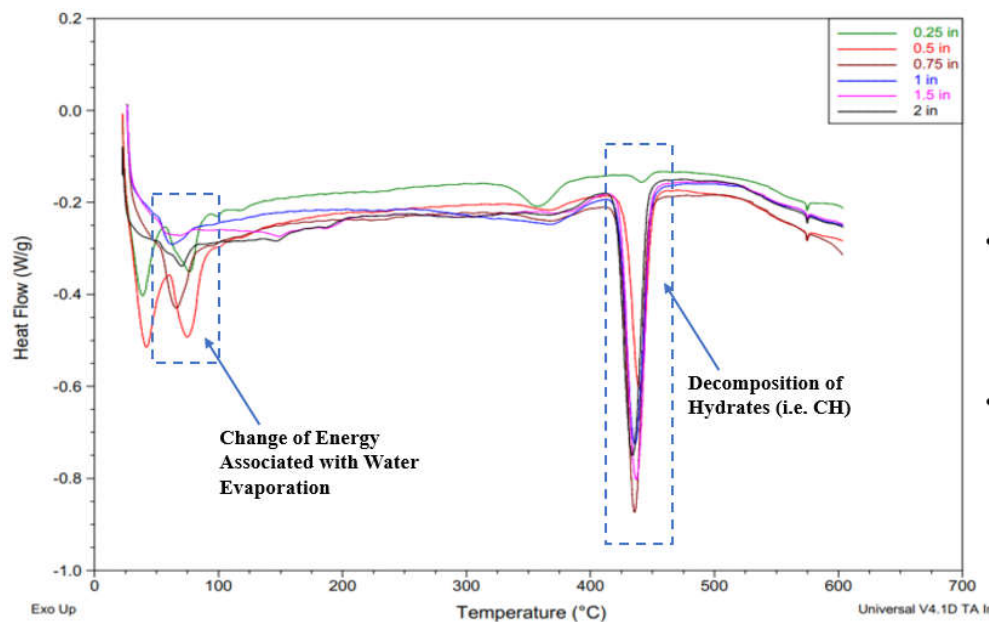
Figure 4-41. DSC Analysis of Heated – 40 Sample

Figure 4-42 shows DSC analysis results of Heated – 80 sample at various depths. Since the peaks of CH decomposition from 0.25 in. to 1 in. depth are significantly smaller compared with Unheated samples, minimal decompositions of CH can be found at and above 1 in. depth. It illustrates that, for 80 minutes heating, the heat has the impact on the composition of CH and concrete strength till and including 1 in. It can also be observed that the amounts of CH decomposed at 0.25 in. and 0.5 in. are higher than those at 0.75 in. and 1 in. It is assumed to be caused by the second effect of in-place rehydration after heating. This fact can be related with the spalling found on the exposed surface after 80 minutes heating. Lime was formed during the heating process by decomposition of calcium carbonate or calcium oxide then reacted with the moisture when spalling happened on the surface after the heating test; eventually resulted as the increase in CH content. However, this could only happen around the surface (i.e. 0.25 in. and 0.5

in. depth), and at 1 in., it is too deep for the moisture going to rehydrate. Similar as Heated – 40 sample, the maximum heat flows for peaks at 100 °C of Heated – 80 are much smaller than the peaks of Unheated sample analysis results, which illustrates the dehydration of Heated – 80 sample up to 2 in. The temperatures for 80 minutes heating at 1.5 in. and 2 in. depth are not high enough to decompose CH, but the temperature up till 2 in. is still adequate to evaporate water during 80 minutes heating test.

Figure 4-42. DSC Analysis of Heated – 80 Sample

Based on Figure 4-40 to Figure 4-42, the content of CH is calculated based on the peak area at corresponding locations, using the calibration equation mentioned above. Table 4-3 summarizes the results of CH content and quantitatively compares the reduction in CH after heating to various time duration.

Table 4-3: Quantitative Estimation of Content of CH for All DSC Samples

Depth (in)	Unheated		Heated - 40			Heated - 80		
	Peak Area (J/g)	CH (%)	Peak Area (J/g)	CH (%)	% Change in CH (%)	Peak Area (J/g)	CH (%)	% Change in CH (%)
0.25	24.13	2.21	1.24	0.11	94.9	2.84	0.26	88.2
0.5	39.18	3.59	34.86	3.20	11.0	8.65	0.79	77.9
0.75	57.30	5.25	55.65	5.10	2.9	1.22	0.11	97.9
1	60.53	5.55	52.02	4.77	14.1	0.84	0.08	98.6
1.5	61.00	5.59	56.73	5.20	7.0	53.56	4.91	12.2
2	58.94	5.40	53.57	4.91	9.1	47.75	4.38	19.0

where *% Change in CH = (CH$_{Unheated}$ – CH$_{Heated}$)/CH$_{Unheated}$ x 100%*

Figure 4-43 shows the content of CH in DSC analysis from all three samples at various depths. As shown in Figure 4-43, CH is decomposed at 0.25 in. for Heated – 40 sample and is decomposed up to and including 1 in. for Heated – 80 sample. As a result, 40 minutes of heating has the impact of CH decomposition to 0.25 in., and 80 minutes of heating has the impact of CH decomposition to 1 in.
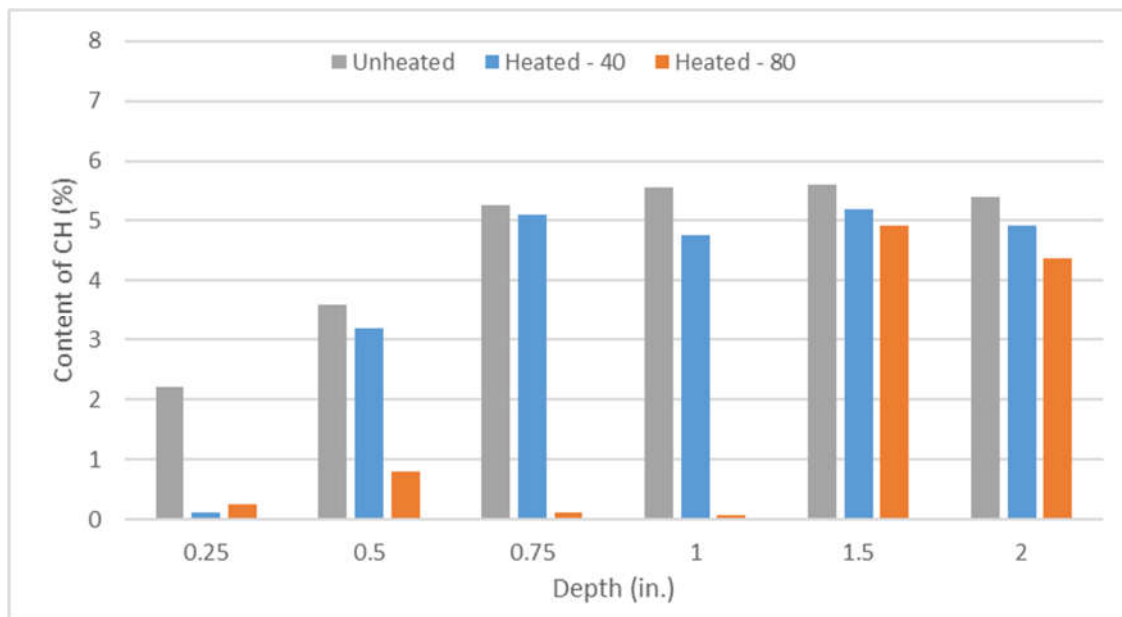
Figure 4-43. Comparison of Content of CH for All DSC Samples

4.4   Summary of Experimental Results

This chapter presented the heating test results conducted to evaluate the thermal and mechanical behavior of concrete deck specimens at elevated temperatures. This chapter also presented the material analysis results conducted to correlate the microstructure degradation by the examination of cored samples from concrete deck specimens prior to and after heating. Two heating tests were targeted to last for various time durations (i.e. 40 minutes and 80 minutes). Several critical parameters were compared from two heating test results. The parameters include cracking and spalling on surface of deck specimen, surface temperature and through-depth temperature profile, deflection of deck specimen, color change of concrete, microstructure degradation of SEM samples, and reduction of content of CH. Several observations and conclusions are drawn from the tests:

- Cracking and spalling on surface of deck specimen: cracks are more visible on the specimen after 80 minutes of heating. Spalling happens after 80 minutes of heating.

- Surface temperature and through-depth temperature profile: temperature results from 80 minutes heating test extend the trends of the 40-minute heating test.

- Deflection of deck specimen: deflection at center of specimen increases with duration of heating. Deflection at quarter span does not change much (<10%) with heating duration.

- Color change of concrete: after 40 minutes of heating, darker grey extends till about 0.25 in. from exposed surface; after 80 minutes of heating, darker grey extends till about 1 in. from exposed surface.

- Microstructure degradation of SEM samples: microstructure degradation (e.g. debonding cracks and increase in porosity) depends on the heating duration and temperature at corresponding location.

- Reduction of content of CH: 95% of CH is decomposed till about 0.25 in. from exposed surface after 40 minutes of heating. 99% of CH is decomposed till about 1 in. from exposed surface after 80 minutes of heating.

The through-depth temperature results from both heating tests are well compared with results from SEM observations and DSC analysis. It can be concluded that during a fire event, the damage caused to concrete extends deeper and gets more severe with exposed temperature and duration increasing.

5. CONCLUSION

5.1 Summary

The purpose of this project is to provide assessment to the concrete bridge deck structures after fire. Both heating experimental tests and material analysis tests were conducted on concrete deck specimens from I-469 over Feighner Road. Two deck specimens were heated for 40 minutes and 80 minutes respectively, with through-depth temperature profiles measured. SEM and DSC analysis were conducted on the concrete samples taken from deck specimens after heating tests. Results from heating tests are well compared with the material analysis results.

5.2 Conclusion

Based on the results from experimental testing, one can conclude that the duration of heating determines temperature through thickness of concrete. If the fire lasts for longer time, temperature through the depth of concrete increases. From the temperature profile through the depth of concrete, the extent of concrete subjected to temperature higher than 752°F (400°C) can then be determined. Based on the observations from material analysis, the portion of concrete that experienced temperature higher than 400 °C loses CH significantly, since the composition of CH is decomposed at this level of temperature. Thus, this portion of concrete would be highly recommended to be replaced with new concrete. When the duration of heating reaches to 40 minutes, 0.25 in. of exposed concrete is compromised by the loss of CH. When the duration of heating reaches to 80 minutes, 1 in. of exposed concrete is compromised by the loss of CH.

5.3   Practical Guidance

Based on the conclusions from this research project, bridge inspectors can establish the associated damage of concrete after fire with knowing the duration of the fire. For practical application of post-fire damage on concrete structures with various types of aggregate, bridge inspectors can take several cored samples from concrete structures at the area that is not exposed to fire to heat the samples to elevated temperature level, and compare them with the cored samples from area exposed to fire, based on the difference between visual observations (such as change of color), in order to develop a brief estimation of the intensity of the fire event. Visual observations like cracking, spalling, and color change can also provide useful information to bridge inspectors about the intensity of fire event.

5.4   Future Work

Recommendations for future work include:

- Fire effect of deck specimens of concrete with more up-to-date concrete mix design or mix design involving fly ash can be a topic to consider.

- Durability of the concrete bridge members should also be studied.

- Repair procedures regarding the observations from this research can be discussed.

LIST OF REFERENCES

Ashraf, W., & Olek, J. (2016). Investigation of the Microstructure of Concrete from the Girders of the Chase Street Overpass. *INDOT Internal Report.*

Ashraf, W., Olek, J., & Jeong, H. (2016). Effects of High Temperature on Carbonated Calcium Silicate Cement (CSC) and Ordinary Portland Cement (OPC) Paste. *5th International Conference on Durability of Concrete Structures, 1-7.* doi: 10.5703/1288284316153

Graybeal, B. A. (2007). Flexural Capacity of Fire-Damaged Prestressed Concrete Box Beams. *Federal Highway Administration. Publication No. FHWA-HRT-07-024.*

Griffin, B., & Beavis, M. (1992). Fire Resistance of Prestressed Concrete. Retrieved July 18, 2019, from https://core.ac.uk/download/pdf/35470325.pdf

Hager, I. (2013). Behaviour of Cement Concrete at High Temperature. *Bulletin of the Polish Academy of Sciences, Technical Sciences.Vol. 61 - 1.*

Hou, X., Zheng, W., & Kodur, V. K.R. (2013). Response of Unbonded Prestressed Concrete Continuous Slabs under Fire Exposure. *Engineering Structures,56*, 2139-2148. doi:10.1016/j.engstruct.2013.08.035

Hou, X., Kodur, V. K.R., & Zheng, W. (2014). Factors Governing the Fire Response of Bonded Prestressed Concrete Continuous Beams. *Materials and Structures (2015) 48:2885–2900,*2885-2900. doi:10.1617/s11527-014-0365-9

Ingham, J. P. (2009). Application of petrographic examination techniques to the assessment of fire-damaged concrete and masonry structures. *Materials Characterization,60*(7), 700-709. doi:10.1016/j.matchar.2008.11.003

Lee, J., Choi, K., & Hong, K. (2010). The Effect of High Temperature on Color and Residual Compressive Strength of Concrete. *Korea Concrete Institute. Fracture Mechanics of Concrete and Concrete Structures. ISBN 978-89-5708-182-2.*

MacLean, K. J. (2007). Post-Fire Assessment of Unbonded Post-Tensioned Concrete Slabs: Strand Deterioration and Prestress Loss. *Master Thesis, Queen's University, Department of Civil Engineering, Canada. 200p.*

MacLean, K. J., Bisby, L. A., & MacDougall, C. C. (2008). Post-Fire Deterioration and Prestress Loss in Steel Tendons used in Post-Tensioned Slabs. *American Concrete Institute. Designing Concrete Structures for Fire Safety, SP-255-7*, 147-174.

Moore, W. L. (2008). Performance of fire-damaged prestressed concrete bridges. *Master Thesis, Department of Civil, Architectural and Environmental Engineering, Missouri University of Science and Technology, United States. 849 p.*

Stoddard, R. (2004). Inspection and Repair of a Fire Damaged Prestressed Girder Bridge. *Pittsburgh: International Bridge Conference. IBC-04-17*. Retrieved July 18, 2019, from http://aspirebridge.com/resources/Stoddard_WA%20Fire_IBC_04.pdf

Zheng, W., & Hou, X. (2008). Experiment and Analysis on the Mechanical Behaviour of PC Simply-Supported Slabs Subjected to Fire. *Advances in Structural Engineering,11*(1), 71-89.